AIAA SciTech Forum
12-16 January 2026, Orlando, FL
AIAA SCITECH 2026 Forum

10.2514/6.2026-2433



# Guidelines and Designs for Helicopter Airfoils and Blades for Mars Applications with Experimental Validation

B. Natalia Perez Perez*, Haley V. Cummings†, Witold J. F. Koning‡, Farid B. Haddad§, Alex L. Sheikman¶, Charles J. Cornelison‖, Alfredo Perez**, Antonio Cervantes††, Stephen J. Wright‡‡, Ethan A. Romander§§, Wayne R. Johnson¶¶, J. Ken Smith***, Ravi Lumba†††, Cheng Chi‡‡‡, Margaret Donovan§§§, Anubhav Datta¶¶¶, Takayuki Nagata[17], Keisuke Asai[18], Taku Nonomura[19], Lidia Caros Roca[20], Oliver Buxton[21], Peter Vincent[22]

**The Rotor Optimization for the Advancement of Mars eXploration (ROAMX) project advances the design and validation of airfoils and blades for next-generation Mars rotorcraft. A comprehensive computational modeling and experimental campaign was conducted to address the unique low-density compressible flight environment of Mars. An airfoil and rotor modeling and optimization framework tailored to Mars Reynolds and Mach number regimes was developed and applied to generate a portfolio of candidate geometries. A novel lift-generation mechanism was identified and experimentally validated, broadening the design space for airfoil and rotor performance. Airfoil performance was rigorously assessed through a combination of wind tunnel testing and high-fidelity computational fluid dynamics simulations under Mars representative flow conditions. Airfoil optimization resulted in airfoils that had a 25% increase in coefficient lift to drag ratio at the 75% radial station, compared to the clf5605 baseline airfoil (Ingenuity Mars Helicopter). Unique internal structural designs were developed to support the unusually thin airfoils, and a structural design methodology for use under the low Lock number environment present for Mars was established. The strength of the rotor blades was verified via static pull testing at 110% of the centrifugal force experienced at a tip Mach number of 0.95. Facilities were expanded at NASA Ames for Mars rotorcraft testing, including the development of a state-of-the-art hover stand capable of high-accuracy performance measurements at very low pressure inside a 30 meter tall chamber of 4,000 cubic meters out of ground effect. Collectively, these efforts culminated in the demonstration of optimized rotor performance at Mars flight conditions, providing validated design tools, test infrastructure, and performance data to support future scientific and exploration rotorcraft missions on Mars. The full-scale ROAMX rotor achieved a 29% increase in peak Figure of Merit over the Ingenuity rotor at design density, with no performance loss at its higher tip Mach number. It also exhibited about 2.3 times lower sensitivity to Reynolds number variation within the range expected for Mars flight.**

*Analytical Mechanics Associates, NASA Ames Research Center, Aerospace and Mechanical Engineer, Moffett Field, CA 94043
†haley.cummings@nasa.gov, NASA Ames Research Center, Mechanical Engineer, Moffett Field, CA 94043
‡Analytical Mechanics Associates, NASA Ames Research Center, Aerospace Engineer,Moffett Field, CA 94043
§United States Air Force, NASA Ames Research Center, Controls Engineer, Moffett Field, CA 94043
¶NASA Ames Research Center, Instrumentation Engineer, Moffett Field, CA 94043
‖NASA Ames Research Center, Aerospace Engineer, Moffett Field, CA 94043
**Jacobs Engineering, NASA Ames Research Center, Engineering Technician, Moffett Field, CA 94043
††NASA Ames Research Center, PAL Facility Manager, Moffett Field, CA 94043
‡‡NASA Ames Research Center, Aerospace Engineer, Moffett Field, CA 94043
§§NASA Ames Research Center, Aerospace Engineer, Moffett Field, CA 94043
¶¶NASA Ames Research Center, Ames Associate, Moffett Field, CA 94043
***Jacobs Engineering, NASA Ames Research Center, PAL Facility Operator, Moffett Field, CA 94043
†††The University of Maryland, Research Associate, College Park, MD 20742
‡‡‡The University of Maryland, Research Associate, College Park, MD 20742
§§§The University of Maryland, Research Associate, College Park, MD 20742
¶¶¶The University of Maryland, Alfred Gessow Professor, College Park, MD 20742
[17]Nagoya University, Assistant Professor, Nagoya, Japan
[18]Tohoku University, Professor Emeritus, Sendai, Japan
[19]Nagoya University, Associate Professor, Nagoya, Japan
[20]Imperial College London, Research Associate, London, England
[21]Imperial College London, Reader, London, England
[22]Imperial College London, Professor, London, England

## Nomenclature

| | | |
|---|---|---|
| $A$ | = | Rotor Area |
| CAMRAD II | = | Comprehensive Analytical Model of Rotorcraft Aerodynamics and Dynamics |
| CFD | = | Computational Fluid Dynamics |
| CG | = | Center of Gravity |
| $C_P$ | = | Coefficient of Power |
| CSD | = | Computational Structural Dynamics |
| $C_T$ | = | Coefficient of Thrust |
| DNS | = | Direct Numerical Simulations |
| ELISA | = | Evolutionary aLgorithm for Iterative Studies of Aeromechanics |
| FM | = | Figure of Merit |
| JPL | = | Jet Propulsion Laboratory |
| NACA | = | National Advisory Committee for Aeronautics |
| $\Omega$ | = | Rotor Rotational Speed |
| $P$ | = | Rotor Power |
| PAL | = | Planetary Aeolian Laboratory |
| PI | = | Proportional-Integral |
| $Q$ | = | Torque |
| $R$ | = | Rotor Radius |
| $\rho$ | = | Air Density |
| ROAMX | = | Rotor Optimization for the Advancement of Mars eXploration |
| $\sigma$ | = | Rotor Solidity |
| SVS | = | Steam Vacuum System |
| $T$ | = | Rotor Thrust |
| UMD | = | The University of Maryland |



## I. Introduction

In 2021, the Ingenuity Mars Helicopter demonstrated powered flight on another planet for the first time by flying on Mars (Figure 1). Ingenuity's sole purpose was to demonstrate that flying on Mars is possible, and far exceeded the expectations for the original five-flight mission, ultimately completing 72 flights which included feats such as serving as scout to the Perseverance Rover. An in-depth investigation of the underlying aerodynamics acting at Mars flight conditions was beyond the scope of the timeline for the development of Ingenuity. At the Reynolds number experienced by Ingenuity on Mars, the Reynolds number is too low to allow for classic laminar separation bubbles or classic boundary layer trips. The approach taken for the design of the Ingenuity airfoils was to maintain a continuous laminar boundary layer on the airfoil, which resulted in a successful flight campaign on Mars. The flow, however, still separates from the airfoils and does not result in a true fully attached laminar boundary layer. Further research was needed to understand the flow physics at these Reynolds numbers to allow for optimization of aerodynamic design to maximize vehicle performance.

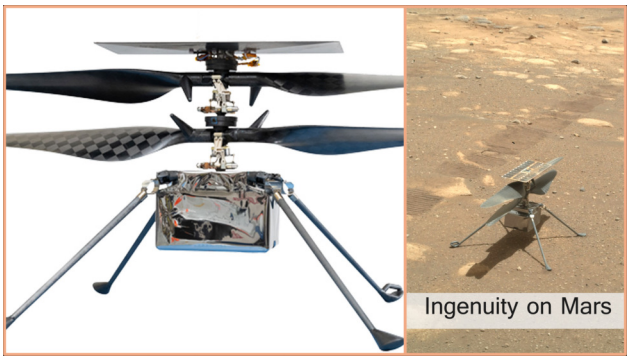


**Fig. 1 Ingenuity Mars Helicopter. Picture from science.nasa.gov.**

The aerodynamic regime in which helicopters fly on Mars is largely unexplored. The low atmospheric density on Mars, which is roughly 1% of that on Earth, results in a Reynolds number that is nearly two orders of magnitude lower than that experienced with flight on Earth (on the order of $10^4$ on Mars, versus $10^6$ on Earth). In addition to the reduced density, the temperature on Mars is much lower than on Earth and the atmosphere is carbon dioxide-based, as opposed to the nitrogen-based atmosphere found on Earth. The combination of the low temperature and carbon dioxide-based atmosphere results in a much lower speed of sound on Mars, on the order of 70% of that on Earth. This results in a higher tip Mach number experienced on Mars for equivalent tip speed (compared to Earth). To compensate for the lack of atmospheric density, the rotor speed must be maximized for an equal-sized rotor, thereby resulting in a high (subsonic) tip Mach number. Thus, on Mars, helicopters fly in a low Re, high subsonic tip Mach number aerodynamic regime that, until recently, was largely unexplored (see Figure 2).

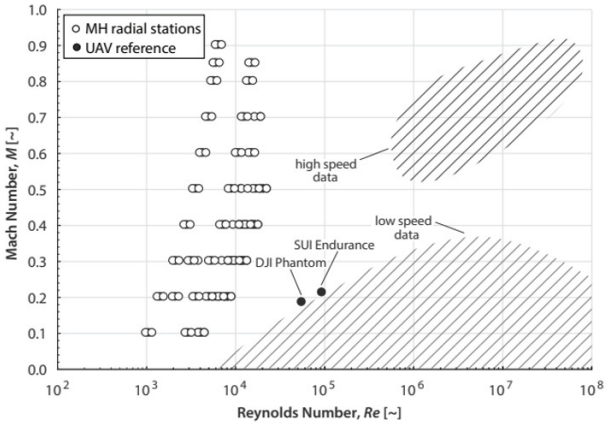


**Fig. 2 Comparison of existing Mach-Reynolds number research regimes with the Mars Helicopter (MH) flight regime [1].**

With aerodynamic design specifically for the low Reynolds number, high (subsonic) tip Mach number flight regime found on Mars, significant improvements in airfoil and rotor performance compared to Ingenuity are possible. The Rotor Optimization for the Advancement of Mars eXploration (ROAMX) project [2, 3] at NASA Ames Research Center sought to increase the understanding of the Mars flight regime, and then utilize that increased understanding to design airfoils and rotor blades optimized for flight on Mars. The ROAMX project computationally optimized airfoils and blades in hover for the low Reynolds, high subsonic tip Mach number aerodynamic regime found on Mars, and experimentally tested the optimized airfoils and full-scale blades. To better assess the performance improvements that were achieved via the optimization, computational analyses and experimental testing was also conducted for Ingenuity's clf5605 airfoil and rotor blades, to serve as baseline and to compare to the ROAMX computational and experimental results.

Blades that exhibit better performance on Mars compared to the blade performance of Ingenuity can enable helicopters that fly farther, faster, and carry significant science payloads on Mars. This leads to more capable helicopter science and exploration missions [4, 5]. Figure 3 demonstrates the impact of increased aerodynamic performance on the overall vehicle performance [6]. Increase in airfoil section lift-to-drag ratio has a multiplicative impact on overall rotor efficiency, or Figure of Merit (FM). In turn, FM has a significant impact on overall vehicle performance. Figure 3 shows hover time and range that is possible for an Ingenuity-sized vehicle that uses ROAMX optimized blades. Notably, the range increases by more than 1200%. The increased aerodynamic performance of the blades allows the vehicle to carry additional payload, which enables a bigger battery for the vehicle, increasing endurance (hover time) and range of the vehicle, as well as increasing scientific payload that the vehicle can carry (whereas Ingenuity was not able to carry a scientific payload). These performance increases are possible with the increased aerodynamic performance provided by the ROAMX optimized airfoils and rotor blades.

## II. The ROAMX Project

This paper summarizes the novel design guidelines and findings developed through the ROAMX project for airfoils and rotor blades optimized for Mars, and presents experimental results from full-scale hover testing comparing the optimized ROAMX blades with Ingenuity's baseline blades. ROAMX was funded by NASA's Science and Technology

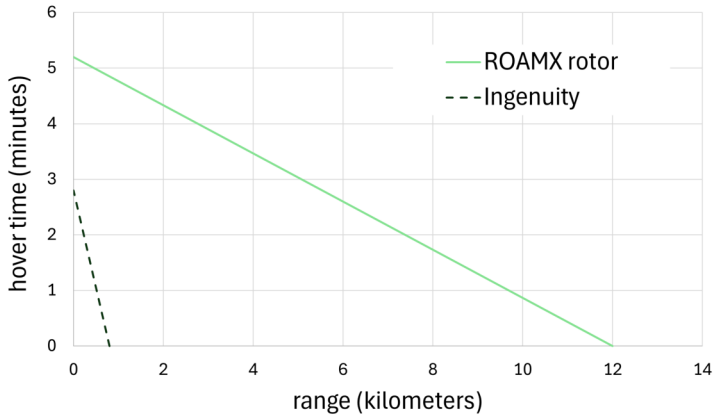


**Fig. 3 Impact on helicopter performance when using optimized blades, compared to Ingenuity [6].**



Mission Directorate through the Early Career Initiative (ECI) program.

The goals of the ROAMX project include:

- Increase the understanding of aerodynamics for flight at Mars aerodynamic conditions (low Reynolds number, high subsonic tip Mach number);
- Develop an airfoil and blade optimization framework that can be used to design airfoils and blades for Mars rotorcraft, given the mission requirements of the helicopter;
- Optimize a rotor blade at Ingenuity's flight conditions to draw a fair comparison of optimized blade performance compared to Ingenuity's baseline blade;
- Utilize high-fidelity OVERFLOW Computational Fluid Dynamics (CFD) and fully resolved PyFR Direct Numerical Simulation (DNS) to verify airfoil performance;
- Experimentally test the Ingenuity and ROAMX representative airfoils;
- Increase the understanding of rotor aeroelasticity for flight on Mars (low Lock number, high centrifugal stresses);
- Investigate the design and fabrication of novel internal structures and root geometries to support the unusual aerodynamic profiles required on Mars and develop design guidelines for future Mars rotors;
- Utilize high-fidelity X3D Computational Structural Dynamics (CSD) to fully resolve hub and blade stresses to verify strength and margins of safety;
- Design, analyze, manufacture, and assemble a test stand capability that can be used to experimentally validate the performance of the Ingenuity and optimized ROAMX blades and provide rapid testing for any future Mars mission blade designs;
- Manufacture an Ingenuity baseline rotor blade set and a ROAMX optimized rotor blade set;
- Enhance the NASA Ames Planetary Aeolian Laboratory (PAL) facility to enable higher quality testing at Mars flight conditions;
- Experimentally test the Ingenuity and ROAMX representative blade sets;
- Develop data acquisition and post-processing algorithms to reduce, analyze, and visualize experimental test data.

All of these goals were met in the project, with significant contributions from many collaborators. The following sections discuss these objectives, and other achievements through the project, in further detail. The results of the full-scale blade experiment are also shown.

### A. Demonstrated Airfoil Modeling Approach Tailored to Mars Helicopter Flight Regimes

An investigation into how airfoils perform at the low Re, high Mach conditions experienced during flight on Mars was conducted via the ROAMX project at NASA Ames Research Center. One of the first outcomes of the ROAMX project was to establish best practices for modeling airfoil performance at these aerodynamic conditions.

Reynolds Averaged Navier-Stokes without the use of a turbulence model applied in the OVERFLOW CFD solver was found to match well when compared to extensive wind tunnel tests conducted on the Eppler 387 airfoil at up to $Re \approx 200,000$ [7, 8]. The study demonstrated that two-dimensional vortex shedding, resulting in unsteady reattachment, can be analyzed using laminar unsteady Navier–Stokes simulations, and that it does not necessitate external disturbances

or three-dimensional instabilities. This study was conducted for 2D airfoils and quasi-3D airfoils (finite span with periodic boundary conditions). The results demonstrated that the agreement between experiment and CFD justified the use of 2D airfoil results under similar aerodynamic conditions, for the design of airfoils and blades, as seen in Figure 4. This result was improved by highlighting updated results from the University of Illinois Urbana-Champaign, indicating the Low-Turbulence Pressure Tunnel (LTPT) turbulent reattachment location was actually the oil-accumulation location instead. This significantly reduced the computational cost of conducting optimization of airfoils to determine the best airfoil shape. As a result, guidelines were established for airfoil designers for this Reynolds number range.

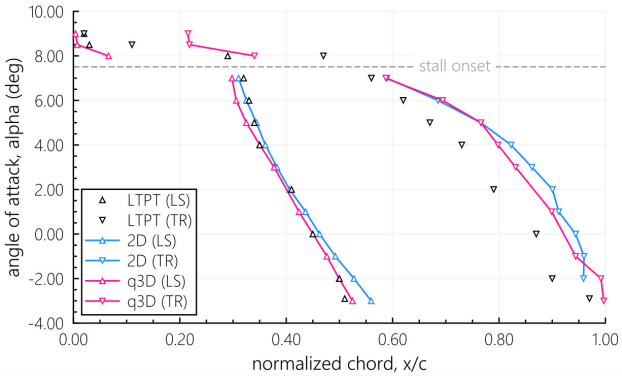


**Fig. 4 Comparing 2D CFD, 3D CFD, and wind tunnel data from the LTPT for Eppler 387 airfoil and demonstrating that 2D CFD matches well for laminar separation (LS) and turbulent reattachment (TR) [7].**

### B. Implemented Advanced Computational Rotor and Airfoil Optimization Frameworks

Using the design guidelines established under the ROAMX project, tools were developed to enable optimal design of airfoils and rotor blades for Mars rotorcraft. The Evolutionary aLgorithm for Iterative Studies of Aeromechanics (ELISA) code parameterizes unconventional airfoil shapes and uses a Genetic Algorithm with multiple objectives and the OVERFLOW CFD solver to provide a Pareto-optimal set of airfoils that have the lowest drag for each given angle of attack [4]. Up to three objectives can be used in the airfoil optimization: lift, drag, and thickness ratio for a given Reynolds number and tip Mach number. Thickness constraints were included to enable optimization with not only aerodynamic but also structural consideration, in order to allow structural designers the latitude to absorb loads and place frequencies. ELISA can optimize airfoils alone, or simultaneously optimize for airfoil(s), planform (chord), and twist distribution to generate the most optimal rotor blade given the mission requirements. For the rotor blade optimization, the ELISA optimization framework optimizes the rotor blade planform and twist for hover using the comprehensive analysis tool Comprehensive Analytical Model of Rotorcraft Aerodynamics and Dynamics (CAMRAD II) by linking the Pareto-optimal airfoil sets for each radial station, as a function of angle of attack, to the rotor optimization. Similarly to the airfoil optimization, the blade optimization is a multi-objective function that seeks to maximize thrust while minimizing power, for a given operating density (Reynolds number). The solidity can be constrained or free and overlapping-blades can be discarded (for high-solidity designs).

The ELISA code sought to study a large range of possible airfoil shapes while not being too computationally expensive and time consuming. The roamx airfoil classes use the notation roamx-$n_c$, $p_c$, $n_t$, $p_t$, where $n$ denotes the number of nodes and $p$ the segment order, with the subscripts c and t referring to the camber and thickness distributions, respectively. This parameterization is used in ELISA; see [6] for a more detailed description. This parameterization allows the designer to choose how complicated of an airfoil shape is desirable (including possible discontinuities along the airfoil profile). Through this feature, the ELISA code was able to generate novel airfoil shapes that demonstrated high performance at Mars aerodynamic conditions, such as those seen in Figure 5. In Figure 5, airfoils at the 50% radial station and outboard are kept at a constant 1% thickness-to-chord ratio, whereas the inboard airfoils use the roamx3-type optimization which includes thickness as the third variable. In this paper, the roamx-0201 airfoil parameterization was used to compare against Ingenuity performance, but ELISA allows for aribtrary roamx- or PARSEC-parameterized airfoils, (see roamx-1301 and roamx-0202, among others).

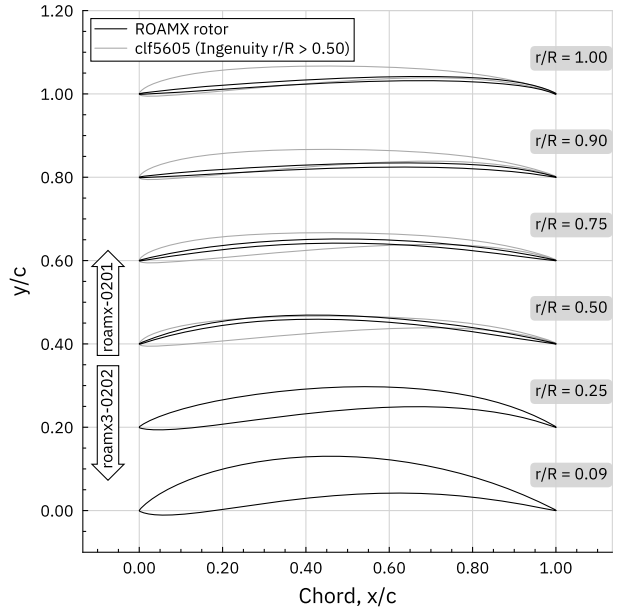


**Fig. 5 ELISA framework used to design the ROAMX blade and airfoils, compared to the Ingenuity airfoils at different radial stations (r/R) [6].**

### C. Designed and Validated Airfoil Portfolio for Mars Flight

The ELISA airfoil design framework outputs a Pareto-optimal set of airfoils for each condition for which an optimization is performed. Figure 6 shows an example of such a Pareto front. This means that the designer can choose, for example, whether to prioritize high lift or low drag for the airfoil that is chosen. The result of this is the generation of an entire family of airfoils with various shapes, representing the lowest drag geometries for each attainable lift coefficient. Through the ROAMX project, the ELISA code was used to generate airfoil shapes for a large range of Reynolds numbers at various thicknesses. This means that future designers should be able to use the ELISA database to choose airfoils for their application, without needing to re-run the ELISA code to optimize the airfoils [9]. Through the ELISA database that was generated, as well as through the speed at which the ELISA code can run to generate new airfoils, the ELISA framework succeeds at enabling the quick turn-around of airfoil and blade design for Mars helicopter applications, depending on the needs of the mission. This was a desired output for the ROAMX project, similarly to how the National Advisory Committee for Aeronautics (NACA) provided airfoil data for various airfoil shapes (albeit on a significantly smaller scale for this project). For access to the ELISA framework or the ELISA airfoil database, please contact the NASA authors.

The airfoil chosen to demonstrate the effectiveness of the ELISA design framework and of the ROAMX project was from the roamx-0201 family of airfoils [4]. The roamx-1301 family of airfoils resulted in markedly higher performance with even more radical airfoil shapes. While the roamx-1301 family of airfoils performed better than the roamx-0201 family of airfoils, short of tests data there were additional uncertainties as to how the airfoil would behave in forward flight due to their unconventional mechanisms of lift generation, or whether such rotor blade structures can be built at all with adequate strength and stability. Therefore, the roamx-0201 family of airfoils was chosen because of the better understood modes of lift generation. Future work includes the experimental testing of airfoils with the unconventional roamx-1301 shape and testing of blades that utilize the roamx-1301 style of airfoils. Such experimental testing can improve knowledge of the lift generation mechanisms and possible increases in performance with these airfoils.

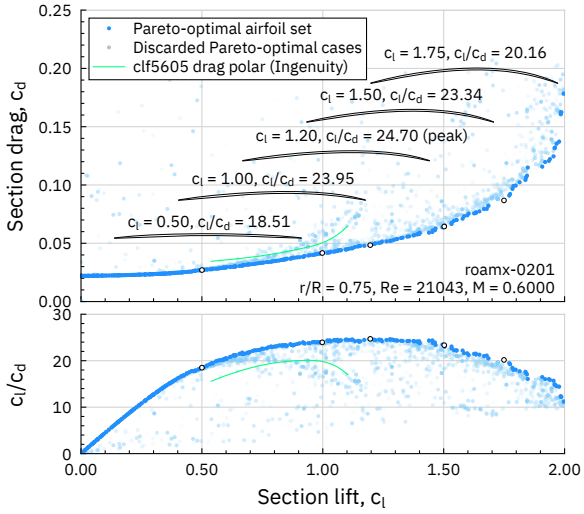


**Fig. 6 Airfoil Pareto front family optimized using ELISA framework [6]. In the images, every dot is a separate airfoil (typically on the order of 100s to 1,000s in one Pareto-optimal airfoil set).**

### D. Novel Lift Generation Approach for Mars Rotorcraft

One of the findings made through the ROAMX project was a novel mechanism of efficient lift generation at these Mars aerodynamic conditions. The roamx-1301 family of airfoils benefits from this novel mechanism. By implementing a sharp leading edge on the airfoil, the separation location is fixed. Large-scale instabilities (in contrast to the small-scale instabilities found in turbulent flow for conventional, Earth-based airfoils) are found to be shed from this separation location and are consistently triggered. The midsection of the airfoil "catches" the flow and causes reattachment of the mean flow. At the very low Reynolds number conditions experienced on Mars, a reattachment of the mean flow is achieved, with vortices that are much larger than traditional turbulent vortices. At low Reynolds number conditions, the viscous forces dominate and transition to turbulence due to instabilities is less likely and more difficult to predict. The sharp leading edge found on the ROAMX airfoils fixes the separation location, resulting in predictable transition location and leading to superior performance at relevant Reynolds numbers, as seen in Figure 7 [4].

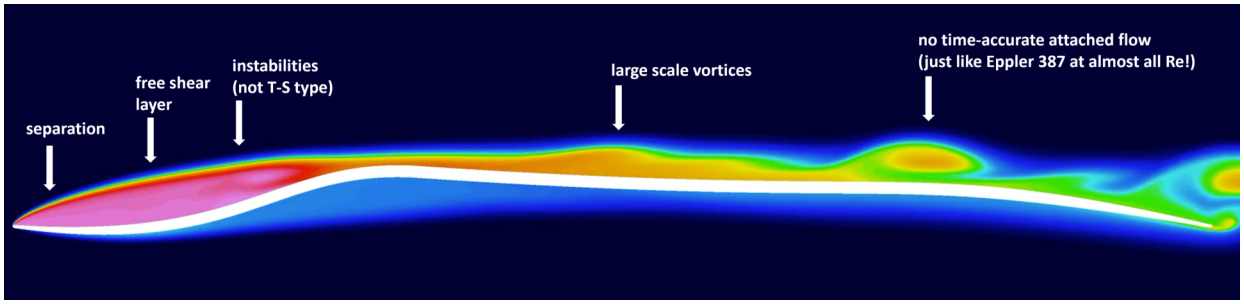


**Fig. 7 The roamx-1301 airfoil with flow features described. The sharp leading edge consistently triggers instabilities, and the dip and subsequent rise allow for the formation of the shear layer and for the airfoil to "catch" and guide the reattachment of the mean flow [6].**

### E. Experimentally Validated Novel Performance Models and Airfoils

To validate the performance of the novel roamx-0201 airfoils, a study was conducted by the ROAMX team in collaboration with Tohoku University, Japan, and Imperial College London. The aim was to conduct performance analysis comparisons between airfoil wind tunnel data collected by Tohoku University with predictions from high-fidelity

CFD using the OVERFLOW solver conducted by the ROAMX team at NASA Ames, and fully-resolved DNS conducted with PyFR by Imperial College London [10]. DNS with PyFR provides a first-principles approach to modeling fluid dynamics by resolving all relevant spatial and temporal scales of turbulence without any turbulence modeling, resulting in the highest possible fidelity flow simulation [10]. The team is shown at the Mars Wind Tunnel at Tohoku University in Figure 8. The Mars Wind Tunnel, previously located at Tohoku University and now located at Nagoya University, is a one-of-a-kind wind tunnel with a small 10 cm by 15 cm test section that allows for testing of airfoils at Re $\sim 10^3$ and high Mach numbers in the compressible flow region ($M \sim 0.6$).

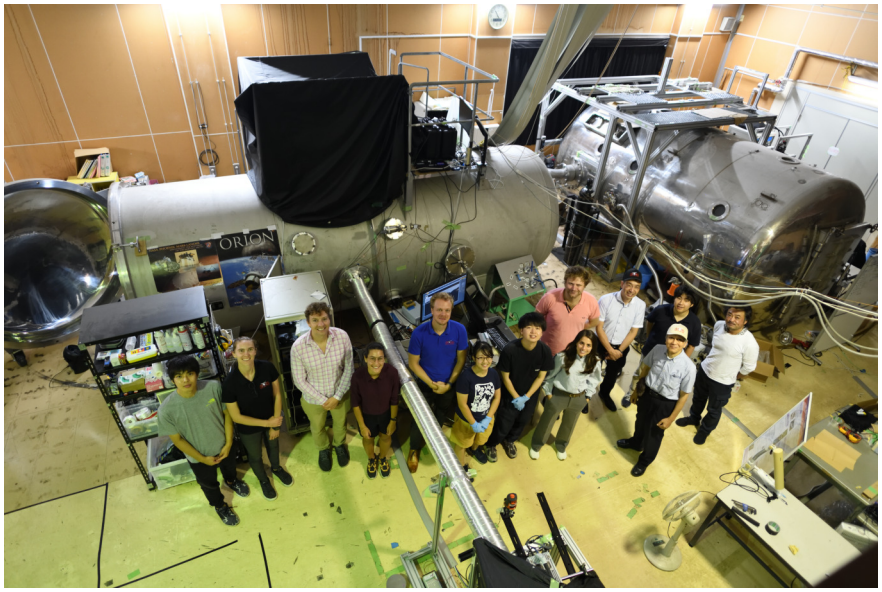


**Fig. 8 Mars Wind Tunnel experimental campaign at Tohoku University. Pictured from right to left: Dr. Keisuke Asai (front - Tohoku), Dr. Takayuki Nagata (back - Tohoku), Dr. Taku Nonomura (Tohoku), Dr. Peter Vincent (back - Imperial), B. Natalia Perez Perez (front - NASA), Yudai Kanzaki (Tohoku), Miku Kasai (Tohoku), Witold Koning (NASA), Dr. Lidia Caros Roca (Imperial), Dr. Oliver Buxton (Imperial), Haley Cummings (NASA), Miku Miyagi (Tohoku).**

Wind tunnel experiments and two numerical approaches, OVERFLOW (approaching Implicit Large Eddy Simulations, ILES) and PyFR (DNS), all demonstrated a significant performance improvement between the roamx-0201 airfoil and the clf5605 airfoil, which was used for Ingenuity, independent of angle of attack, as seen in Figure 9 [11]. The Ingenuity clf5605 airfoil is referenced as the baseline for this study, as that airfoil was the state-of-the-art at the commencement of this research. Caros et al. [11] shows that the roamx-0201 airfoil is able to achieve approximately 25% higher lift than the clf5605 airfoil (at equal drag). This result is shown in Figure 9e. The drag polars for all analysis methods furthermore demonstrate that the roamx-0201 profile exhibits lower drag compared to the clf5605 for all angles of attack. The performance increase for the optimized airfoils validates the case for using unconventional, optimized airfoils for future Mars helicopters. The conceptual design vehicle being developed at NASA's the Jet Propulsion Laboratory (JPL) for future Mars missions, Chopper, is using ROAMX/ELISA optimized airfoils and blades [12, 13]. In addition, other studies have incorporated ROAMX airfoils into conceptual design analyses, including [14], which used the airfoils in a long-range Mars helicopter concept study.

### F. Implemented Performance Enhancement Strategies into Rotor Optimization

Because of the significantly reduced density of the atmosphere on Mars, generating lift is more difficult than on Earth. There are several ways additional lift can be generated by helicopters on Mars including: (1) utilizing more efficient airfoil technology for low Reynolds and high Mach number flow; (2) increasing rotor speed; and (3) increasing rotor solidity (i.e. increasing blade area for a fixed rotor diameter). Helicopters traveling to Mars have to fit inside a fixed aeroshell size, thereby limiting the rotor radius that can be used. Thus, to increase blade area, the solidity of the rotors must be increased beyond conventional solidities used for Earth-based helicopters. For the design of the ROAMX blades, all three of these parameters were leveraged. Airfoils were designed to have superior performance for the low

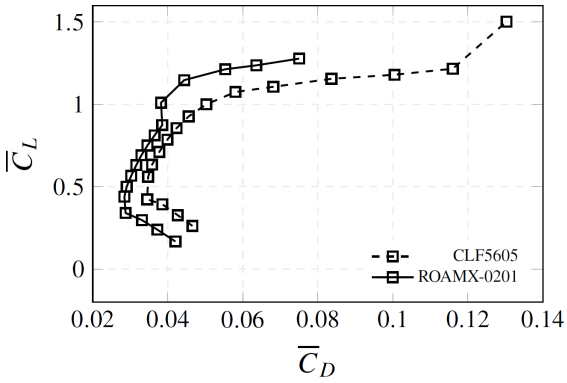


**(a) OVERFLOW 2D.**

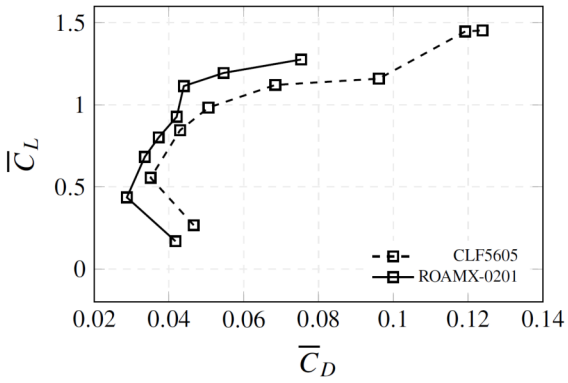


**(b) PyFR DNS 2D.**

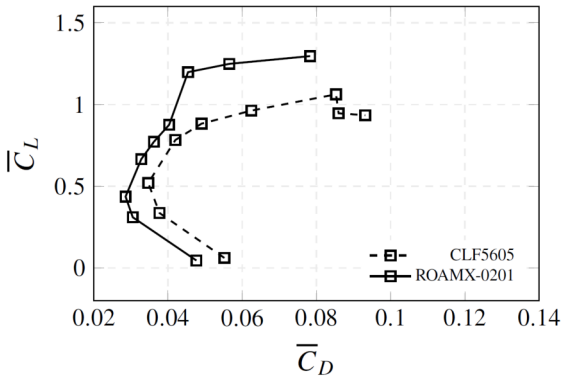


**(c) OVERFLOW 3D spanwise periodic.**

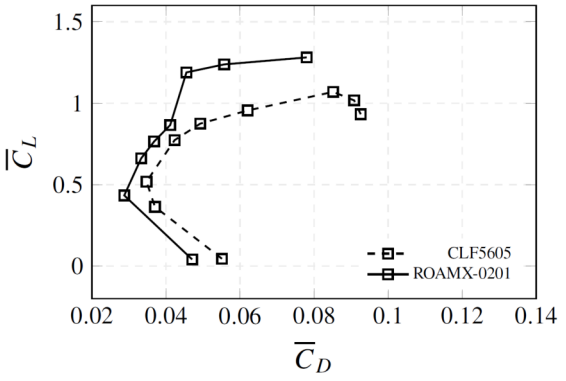


**(d) PyFR DNS 3D spanwise periodic.**

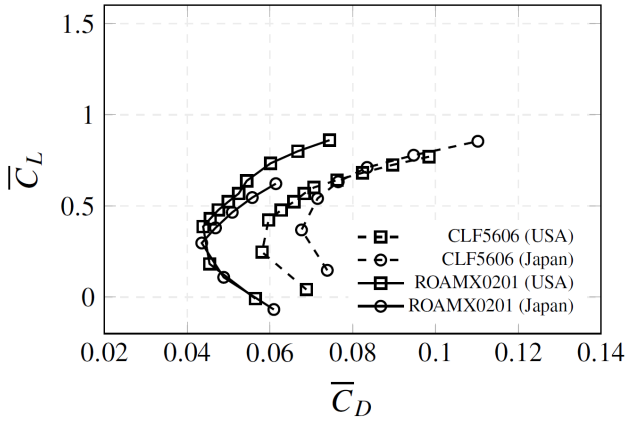


**(e) Mars Wind Tunnel experiments. "Japan" and "USA" refer to where the airfoil was manufactured.**

**Fig. 9 Comparison of average coefficient of lift ($\overline{C}_L$) vs average coefficient of drag ($\overline{C}_D$) for roamx-0201 and clf5605 airfoils using OVERFLOW 2D and 3D, PyFR DNS 2D and 3D, and experiment [11].**

Reynolds, high Mach regime up to near sonic speeds (up to $M \sim 0.95$ ). The solidity of the rotor was also increased beyond conventional solidities (for example, Ingenuity's rotor has a solidity of 0.148 [5]). Research is limited in the area of high solidity rotors since Earth-based helicopters favor increasing radius to increase thrust, and the aerodynamic effects of increasing solidity to very high values (above solidity of 0.3) are not well understood. The ROAMX rotor was chosen to have a 6-bladed rotor with a solidity of 0.25, to modestly increase the solidity beyond conventional solidities (which are well understood) while staying in a conservative range of high solidity. Future helicopters for Mars will need to employ even higher solidity rotors to be able to further increase lift and range capabilities. Research has started at NASA Ames to investigate these higher solidity rotors. To compare against the Ingenuity blade performance, which was used as the baseline, the ROAMX rotor was optimized using the same rotor radius and flight conditions as Ingenuity. For aerodynamic performance, the parameters of interest to match are the Reynolds number and tip Mach number. To generate the ROAMX optimized rotor blade, airfoils were optimized for several radial stations along the blade, with higher thickness ratio blades of type roamx-0202 (type roamx-0202 airfoils have a thickness degree of freedom in the optimization) used inboard to provide structural support, and 1% thick roamx-0201 airfoils used at the 50% radial station and outboard. The airfoils are novel in their shape, with a sharp leading edge that immediately separates and trips the boundary layer and enables the large-scale instabilities to develop; the overall shape of the roamx-0201 airfoils is closer to the shape of a cambered flat plate than a typical airfoil used on Earth. The airfoils are also only 1% thick to mitigate the impact of flying at high subsonic tip Mach number. Even with these aerodynamic improvements, the structural weight must still be reduced, and it must begin with the rotor.

### G. Established Structural Design Framework for Mars Flight Applications

The structural design of the ROAMX blade was performed in a collaboration with the University of Maryland (UMD). The design covered the blade, root, and adapter. The challenge was to design a structure that could support the unusually thin 1% thickness to chord ratio aerodynamic profile without undesired deformations, absorb loads with adequate stress margin, harness sufficient aeroelastic damping for stability, and be manufacturable without surface wrinkling and resin bubbling, all within a strict weight budget. Adequate flapping frequency needed for control was also ensured, although it was not critical to the ROAMX tests.

The ultra-low density on Mars (low Lock number) was exploited to meet a number of these challenges. The low Lock number reduces aeroelastic sampling between modes and mitigates flutter. Therefore, leading-edge weights, needed on Earth to bring the center of gravity (CG) at or ahead of the aerodynamic center could be eliminated. Note, however, even though the coupling is reduced, the modes individually remain lowly damped, with the danger of sustained oscillatory motions in response to any perturbations. Low density also meant inertial loading was dominant over aerodynamic loading. Therefore, the pitch axis could be moved back without severe repercussions on the control loads as on Earth. This provided latitude for an innovative internal spar construction that was balanced about the pitch axis without large CG offset and allowed the 1% thickness to chord ratio profile to be supported. The absence of large CG offset also eradicated the need for counter-weights like Ingenuity used.

The rotor blade aerodynamic shape and outer mold line were specified by the ROAMX team and generated using the ELISA optimization framework. The profile outboard of 50% radial station was maintained at all costs. The profile inboard was modified, collaboratively, to account for blade retention, stress concentrations, margins of safety, placement of the pitch axis, and requirements of internal ply layup to construct the unusual spar. UMD designed and analyzed the blade using their 3-dimensional Finite Elements Analysis (FEA) based rotor solver, X3D [15]. The X3D solver was validated for blades used on Earth, as seen in Figure 10, as well as for blades for Mars and provides a unique, rotating, 3D structural analysis for the blades [16–21]. The deformation and loads on ultra-thin rotors with twist and varying sections are governed by an interesting interplay of trapeze effect, propeller moment, pitch angle, pitch axis, CG, and centrifugal stresses. Significant elastic twist, of 5 degrees or more, were predicted at the tip of the blades. These, along with spanwise discontinuities in materials and geometry warranted a 3-dimensional FEA based rotor analysis.

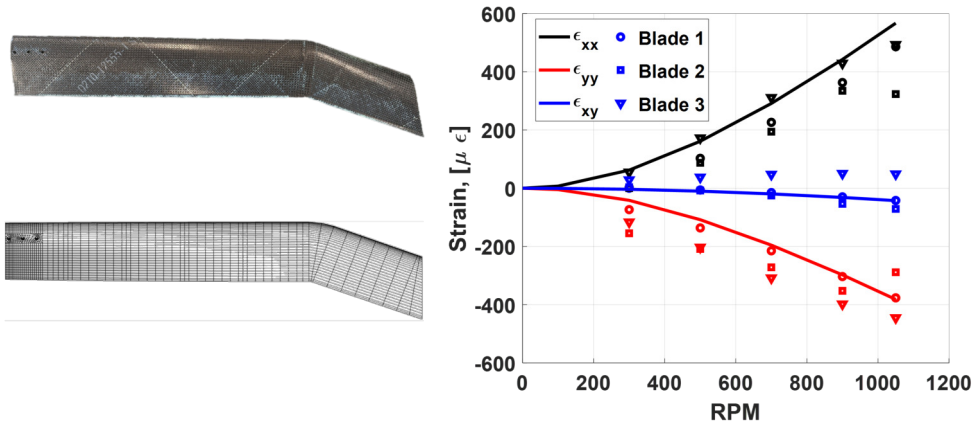


**Fig. 10 X3D validation case; left: manufactured swept tip blade and X3D mesh model; right: mean surface strain of swept tip blade - experiments (symbols) versus X3D predictions (solid line) [19].**

UMD ensured that the blades met NASA wind tunnel model criteria for the structural design and analysis of the blades. The blade structure was designed to have a safety factor of 2 when spinning at a maximum speed of $M_{tip} = 0.95$ and a maximum collective of 20 degrees. UMD also obtained sample coupons of the carbon fiber material from which the blades were manufactured to ensure proper structural properties of the material could be used in their analyses. The blades were manufactured using the carbon fiber ply layup specified by UMD, shown in Figure 11. Sensenich Propellers, Inc. fabricated the optimized ROAMX blades, as well as an aerodynamic replica of the Ingenuity blades. The ROAMX optimized blades were non-destructively tested via centrifugal pull test prior to experimental testing [22].

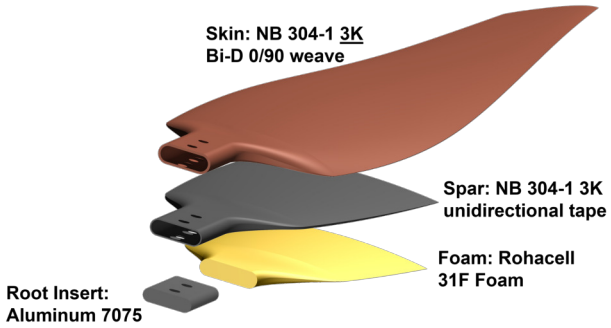


**Fig. 11 Carbon fiber layup for ROAMX blade, specified by UMD [16].**

UMD noted that at the design condition, the aerodynamic loads are negligible compared to the inertial loads experienced by the blade, simplifying the fluid-structure coupled analysis process by partially decoupling the aerodynamic and structural design.

A major load on the thin blade structure is the torsion moment, which is dominated by the inertial loads on Mars. Conventional blade design involves having the pitch axis at or ahead of the aerodynamic center, which usually near 25% chord (quarter-chord), including the Ingenuity rotor. UMD took an innovative design approach for the ROAMX blades and moved the pitch axis to 40% chord, significantly reducing the pitch loads, as well as tensile and compressive loads on the blade, as seen in Figure 12. 40% chord was selected for the pitch axis as a favorable trade-off between reducing structural stress and maintaining aeroelastic stability margin. Moving the pitch axis to 40% chord increased the structural margins for the blades, as seen in Figure 12, allowing for the potential of spinning the blades at higher speeds or using lighter, thinner materials. This is particularly important for Mars, as this can lead to weight reductions and structural optimization. Future designs of blades for Mars helicopters can benefit from this shift of the pitch axis, as it not only reduces stress on the blades but also reduces the pitch loads, further decreasing the strength and weight requirements for the pitch mechanism, and reducing the power requirements for the pitch actuators. The thin ROAMX blades (with 1% thick airfoils from 50% radial station) were successfully manufactured and statically tested. The UMD

X3D solver was successfully utilized to design novel shaped blades under novel conditions. The details of this structural design is documented in [16].

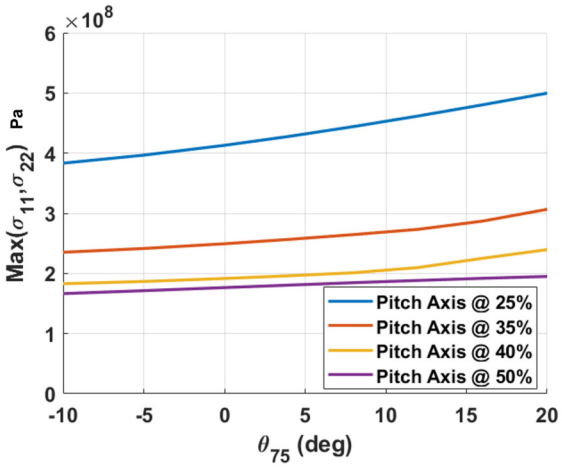


**Fig. 12 Reduction of stress in the blade possible by shifting the pitch-axis location along the chord, defined as a percentage of chord length measured from the leading edge [16]. The y-axis shows the maximum stress on the blade and the y-axis shows the pitch angle at the 75% radial station.**

### H. Static Blade Pull Test Stand Implemented and Validated with Successful Load Tests

The ROAMX blades are experimental blades and the first of their kind to be tested. Thus, efforts were conducted to demonstrate their structural strength prior to spinning the blades. Since the inertial loads dominate the aerodynamic loads, the critical load during spinning of the blades comes from the centrifugal force. A test stand to conduct a static pull test was developed and a static pull test was performed at 110% of the centrifugal force experienced at a tip Mach number of 0.95, resulting in a total applied load of 2,716 lb [22]. There is a major stress at the root of the blade near the retention mechanism. The static pull test validated that the retention mechanism could withstand the high centrifugal loading force. The static pull test was conducted, and no structural damage was observed on the blade, thus validating the structural design conducted by UMD.

### I. Facility Expansion for Expanded Mars Test Capability

To replicate the aerodynamic flight conditions experienced on Mars, a low-pressure chamber was required and to mitigate the effect of recirculation, a large chamber was required. The Planetary Aeolian Laboratory (PAL) at NASA Ames Research Center was chosen for the test [23]. The facility is a 4,000 cubic meter volume facility with a height of 30 meters. It was originally designed to conduct vibration testing on rockets in the 1960s. The facility can pump down to pressures of approximately 5 millibars. By varying the pressure in the chamber, the density can be varied and thus the Reynolds number the rotors would experience on Mars can be matched.

The PAL utilizes the NASA Ames Steam Vacuum System (SVS) to provide vacuum to the chamber. The SVS is part of NASA Ames Arc Jet Facilities infrastructure. The SVS is able to remove a majority of the air from the 4,000 cubic meter volume of the PAL in about 45 minutes. Through the ROAMX project, the PAL facility was upgraded so that it can maintain steady pressure while testing. Previously, as the facility was made to test rockets, the valve that connects the PAL to the SVS was controlled by two push buttons that would either open or close the valve. For Mars rotorcraft testing applications, this made it very difficult to maintain a steady pressure in the PAL chamber, which is necessary to take accurate aerodynamic measurements. A Proportional-Integral (PI) controller was implemented on the pressure valve such that it can read the absolute pressure of the facility and automatically control the valve to achieve the user's specified pressure. A system checkout test is shown in Figure 13.

With this upgrade, the controller can maintain exceptional pressure regulation within +/- 0.05 mbar in the 4,000 cubic meter facility for the duration of the test. Before the upgrades, pressure was difficult to maintain steadily, and it took tens of minutes to arrive at a steady pressure. With the implementation of the new control system, the pressure can be maintained steadily within around 1 minute, as shown in Figure 14.

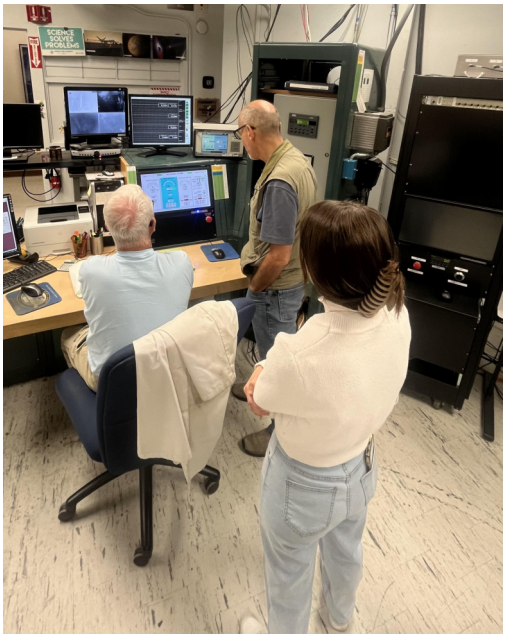


**Fig. 13 Checkout test of the PI controller to control pressure in the PAL facility.**

The graph on the left of Figure 14 shows data from a 2018 test in which the facility attempted to maintain a steady pressure near 12 mbar. During that test, stable conditions suitable for high-quality data collection were not achieved until roughly one hour after pressure regulation began. Following the pressure-control system upgrades implemented by the ROAMX project, the 4,000 cubic meter facility can now reach steady-state pressure within minutes of initiating regulation—rather than after an hour. Moreover, the new control process is fully repeatable, replacing the previous manual regulation that depended on operator skill in adjusting a valve. With this upgraded system, pressures at all Mars-like conditions can now be maintained within 0.05 mbar of the target value.

This is particularly important as the time which the PAL is connected to the SVS is limited, and on average windows of opportunity for the PAL to access vacuum are around 40-60 minutes. Previously, half of that time was spent just setting on a condition; now that time can be used for collecting research data [24]. This upgrade not only allows for high quality aerodynamic test measurements to be taken, it also opens the possibility for additional testing in the PAL, such as forward flight rotor testing using air injectors. The air injectors are required to generate wind speeds to test forward flight as fans do not perform well at low densities. Regulating pressure with air injection is now possible with the PI controller that has been implemented. Similarly, the PAL has been used to test Mid-Air Helicopter Deployment representative jet packs which also exhaust air [25]. The ability to maintain pressure for this testing was also made possible with the PI controller implemented through the ROAMX project.

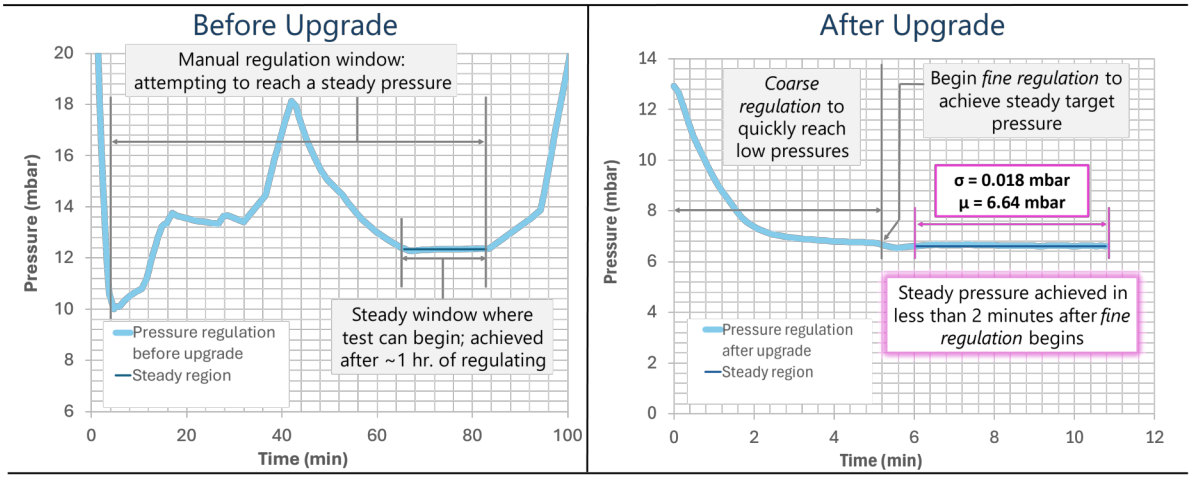


**Fig. 14 Achieving steady facility pressure before and after ROAMX upgrades to the PAL pressure control system.**

## III. ROAMX Hover Stand Developed and Tested for Future Research

The ROAMX experimental test stand, shown in Figure 15, was designed to be used in the PAL at NASA Ames Research Center. Test stand specifications are shown in Table 1. It was designed as a hover test stand that maintains the rotor two rotor diameters above the ground to avoid in-ground effects. The diameter of the stand was kept to less than 20% of the rotor diameter to reduce blockage. The test stand incorporates strain gauge sensors to quantify blade performance. Some of the sensors are shown in Figure 17 and sensor specifications are shown in Table 2. Because the test stand was designed to test experimental rotors, features were built into it to so that it can sustain blade out without damaging the test stand hardware. Wind tunnel model mechanical design requirements mandate that, in general, a safety factor of one over ultimate strength is maintained under loads experienced in blade out, which is when a blade breaks or is lost during testing. In this case, the test stand was designed to have safety factors of two over yield strength under blade out loads. A swivel joint mechanism was included such that if a blade out occurred, the swivel joints would bear the blade out load and protect the rest of the stand hardware. The swivel joints are not engaged during normal operation. No blade outs have been experienced during testing for the ROAMX test campaigns.

The goal of the development of the test stand was to allow for measuring blade aerodynamic performance for current and future Mars blade designs with minimal hardware development efforts required; as such, it was desired to select a strong hub that could be used for an extended period of time. The selected hub is a 4-bladed variable pitch propeller hub manufactured by DUC Helices, shown in Figure 16. This DUC hub has high ratings for centrifugal loading, thrust, pitch load, and side force, and is used in flight on airplanes with thousands of hours of flight time [26]. The centrifugal loading capacity of the DUC hub far exceeds the loads experienced on the ROAMX stand. Because the test stand is designed for ideal hover, cyclic control was not required.

### A. Sensors for Monitoring

Rotor performance measurements were collected via strain gauge sensors. Three Interface SM-100 load cells were used to collect thrust measurements, and an Interface TCSF-50NM torque sensor was used to collect torque measurements. Three triaxial Michigan Scientific TR3D-B-250 load cells were used as part of the Safety of Flight monitoring system to monitor side forces. Thermocouples were affixed to the load cells to monitor temperature drift. Two RPM sensors were used – one was an Omron E3S-AR11 optical sensor combined with retro-reflective tape, and the other was an encoder internal to the motor. A summary of the sensors used can be seen in Table 2. An end-to-end calibration was performed on the sensors that collected performance data using the full cable lengths, bulkhead pass-throughs from ambient to vacuum, and amplifiers in place. Check loads were conducted before and after each test run to ensure the accuracy of the sensors was maintained throughout the test.

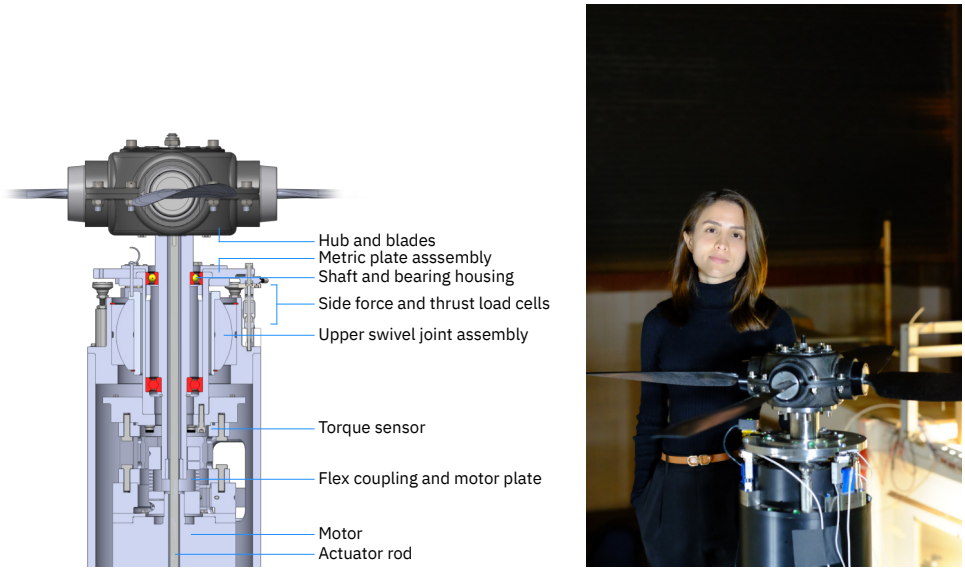


**(a) ROAMX test stand cross-section with component callouts.**

**(b) ROAMX stand with ROAMX blades installed in the PAL at NASA Ames Research Center.**

**Fig. 15 ROAMX experimental test stand CAD and installation in the PAL.**

**Table 1 Summary of Performance Specifications for ROAMX Hover Test Stand.**

| Feature | Specification / Description |
|---|---|
| Hover Test Condition | Rotor plane is greater than two diameters away from the ground. |
| Motor Cooling | Water-cooled motor allows for continuous testing without risk of overheating (convection cooling of motor is not possible at Mars densities). |
| Continuous Rated Torque and RPM | 83 Nm at 5900 revolutions per minute (RPM). |
| Sensors | High-accuracy sensors collect performance data (Figure 17).<br>*Thrust:* Three uniaxial Interface SM-100 load cells, ±0.03% full-scale nonlinearity, ±0.01% full-scale nonrepeatability, 440 N full-scale each.<br>*Torque:* Interface TSCF-50, 0.1% accuracy, 50 Nm full-scale. |
| Safety Factor | $>$ 11 over yield strength under normal operating conditions (higher load capacity possible with future analysis). |
| Normal Operating Conditions | Thrust: 300 N.<br>Torque: 50 Nm. |
| Hub Capability | 27° collective range.<br>Supports single-rotor testing in two- or four-blade configurations.<br>Single-rotor tests relevant for future Mars helicopters (e.g., hexacopters). |
| Structural Capacity | Withstands and continues operation after blade-out loads of 10 kN. |
| Balancing | Built-in weight attachment locations on shaft for blade balancing. |
| Blade Swapping | Hub allows easy swapping of blade sets to allow for testing of different blades. |
| Shaft Interface | ROTAX flange shaft allows use of different hubs. |
| Test Environment | Operates at pressures from 1020 mbar to 5.5 mbar.<br>All components are vacuum-rated and suitable for Earth pressures, enabling testing across a wide Reynolds number range. |

**Fig. 16 Ingenuity and ROAMX blades installed on DUC hub.**


**(a) Interface TSCF-50NM torque sensor.** **(b) Interface SM-100 thrust sensor.** **(c) Omron E3S-A optical RPM sensor.**

**Fig. 17 Torque, thrust, and RPM sensors used in the ROAMX test stand.**

**Table 2 Sensors used in the ROAMX test.**

| Sensor Use | Sensor Name |
|---|---|
| Thrust Measurement | Interface SM-100-1357 (±0.03% full-scale nonlinearity, ±0.01% full-scale nonrepeatability) |
| Torque Measurement | Interface TCSF-50NM (0.1% accuracy) |
| Side Force Monitoring Measurement | Michigan Scientific TR3D-B-250 |
| RPM Sensor | Omron E3S-AR11 |
| Temperature Measurement | Evolution P3A-TAPE-REC-PX-1-PFXX |
| Primary Pressure Measurement | Mensor CPC6000 Pressure Calibrator |
| Secondary Pressure Measurement | MKS627H |
| Environment Temperature and Humidity Sensor | Vaisala HMT300 |

## B. Sensor Accuracy Checks

In addition to the in-place calibration, additional checks were performed for the thrust and torque sensors to ensure their accuracy during testing. The intention was to apply a known load as it is applied during the test (at the rotor plane) to check the system as a whole as it is used in the final experimental configuration. The system was verified in this manner for the sensors used to measure thrust and torque.

To check the torque sensor, an inline rotary torque sensor (reference rotary torque sensor) was installed on top of the shaft and the test stand motor was used to provide torque to both the performance torque sensor and the reference rotary torque sensor. Both torque sensors show agreement within a standard deviation of 0.009 Nm for 51 data points. Setup and results for the torque check can be seen in Figure 18. The reference rotary torque sensor is a Futek TRS300 with nonlinearity and nonrepeatability of 0.2% of rated output each, and a hysteresis of 0.1% of rated output.

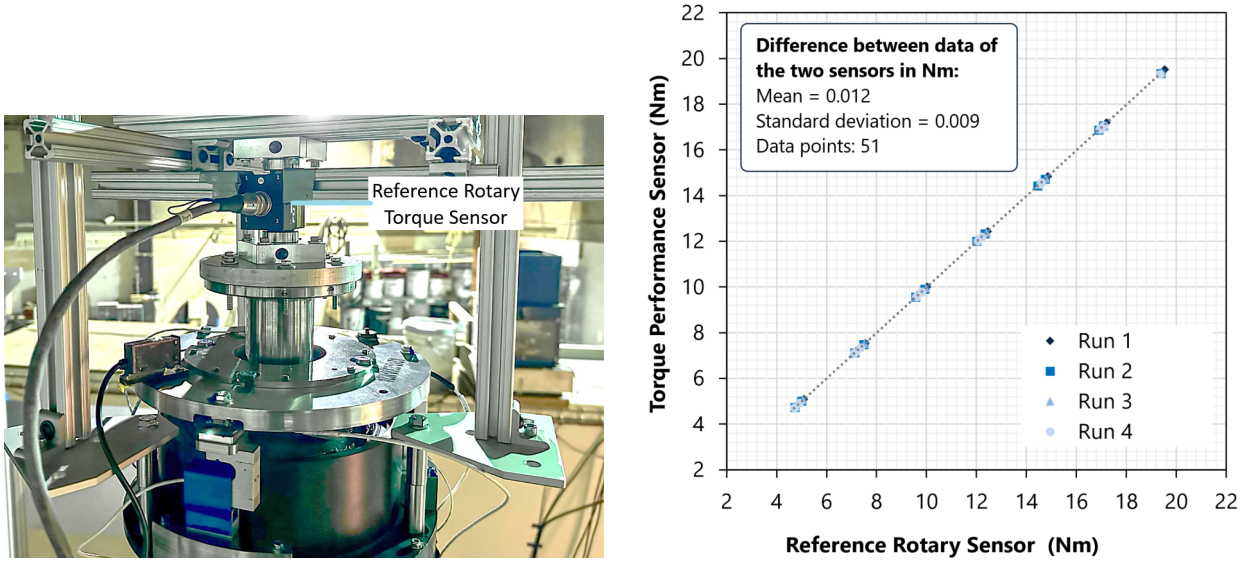


**(a) Torque accuracy check setup with reference rotary torque sensor installed above shaft.**

**(b) Results from torque check showing agreement between performance torque sensor and reference rotary torque sensor.**

**Fig. 18 Torque check setup and results.**

To check the thrust load cells dynamically, a third rotor (AWT propeller) was tested on the hover test stand at normal atmospheric conditions. This two-bladed propeller has previously been tested by NASA on a different hover stand, with different sensors, and the thrust values per RPM are known. The thrust values measured by the ROAMX performance thrust sensors showed good agreement with the previously measured thrust performance [24]. The standard deviation for 33 data points was 0.63 N. Setup and results for the thrust check can be seen in Figure 19.

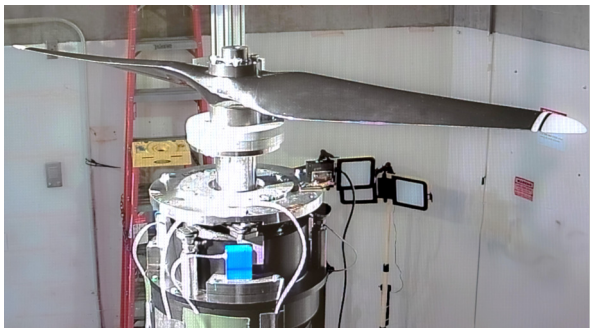

**(a) Thrust check setup with AWT propeller installed on shaft of ROAMX stand.**

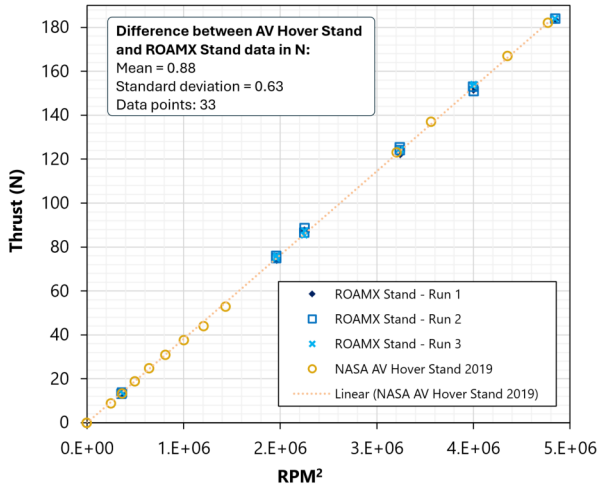


**(b) Results from thrust check showing agreement between AWT propeller performance on ROAMX stand and other test stand.**

**Fig. 19 Thrust check setup and results.**

### C. RPM Control

The test stand RPM is controlled from inside the control room, as seen in Figure 20. The pilot has a dedicated screen where the RPM readout is displayed. The maximum RPM limit can be digitally set, and the maximum RPM is tied to a switch that disengages motor power if the limit is exceeded. The potentiometer controller RPM is also tuned such that the minimum RPM it can provide is 0 and the maximum RPM it can provide is 4300 RPM. In addition, for safety of flight, an intentional limit was set on the motor drive for maximum current, such that at normal operations, the motor would not exceed 45 Nm of torque provided. These three measures are implemented to ensure the test stand cannot exceed safety limits which are determined such that mechanical limits on the test stand and blades are not exceeded.

**Fig. 20 Control console, potentiometer, and RPM display for rotor.**

### D. Data Acquisition System

The sensor cables were connected to bulkheads on the vacuum and ambient sides of the test facility and were connected to an AstroNova TMX data acquisition system in the control room (shown in Figure 21). The sampling rate for all sensors was set at 5,000 Hz. Data was acquired continuously throughout each run, which consisted of an RPM sweep at a set collective angle. Zero points were taken at the beginning and end of each run to account for temperature drift throughout the run. The time for each run varied depending on how many data points were taken. On average, each run took approximately 4 minutes.

**Fig. 21 TMX data acquisition system during system checkouts.**

## IV. Characterized Blade Performance at Mars Flight Conditions

The primary goal of the full-scale rotor experiment was to compare the performance of the Ingenuity and ROAMX blades at their respective design conditions. The Ingenuity blades and ROAMX blades had identical radii for the experiment. The Ingenuity blades have exactly the same geometry as flown on Mars. The shape of the Ingenuity blade was obtained from JPL. The blades were tested in a four-bladed single rotor configuration in hover because of the commercial availability of four-bladed hubs. The ROAMX rotor was optimized as a six-bladed configuration with solidity of 0.25, whereas the rotor was tested in a 4-bladed configuration, resulting in a solidity of 0.167. The Ingenuity rotor was tested in an identical four-bladed single-rotor configuration, resulting in a solidity of 0.148, matching the solidity value used during Mars flight.

The parameters matched during the experiment were the tip Mach number and the Reynolds number experienced by the Ingenuity blades on Mars. Tip Mach number and Reynolds number can be matched by varying the RPM of the rotors and by varying the pressure in the chamber. The Ingenuity design flight tip speed was $M_{tip} = 0.7$. The ROAMX design tip Mach number $M_{tip} = 0.8$. The aerodynamic replica of the Ingenuity blades which were tested were structurally designed to be operated near their design conditions for this experiment, and their operation was thus limited to that speed. A lightly damped structural mode of the test stand was identified at $M_{tip} = 0.7$, so the blades were spun at $M_{tip} = 0.74$. The ROAMX blades are designed to reach high subsonic tip speeds without experiencing significant adverse effects due to nearing the speed of sound. The ROAMX blades were spun at both $M_{tip} = 0.74$ and $M_{tip} = 0.8$ to compare against Ingenuity; the ROAMX blades are designed to be able to be spun at an even higher tip Mach number to generate more lift, but spinning beyond $M_{tip} = 0.8$ was beyond the scope of the current test campaign. Several density conditions were tested to characterize the blade performance over the range of densities experienced on Mars. This was done to investigate the impact of Reynolds number on blade performance. Carbon dioxide was not used during the test; experiments at Tohoku University showed that there is little aerodynamic impact from using carbon dioxide versus Earth air [27].

### A. Experimental Test Procedure

The preparation to spin the experimental ROAMX and Ingenuity blades was a multi-step process. During the build-up of the test stand, ground vibration testing was conducted to identify the natural frequencies associated with lightly-damped structural modes of the test stand that might be excited by the rotor during operation. To avoid excitation of these modes, a "no dwell" band of RPMs was defined for each potentially excitable mode, and these bands of RPMs were avoided during testing. Figure 22 shows the ground vibration test being executed.

NASA wind tunnel model test criteria require that the blades be spun to 110% of the desired test RPM prior to installation in the NASA wind tunnel. The ROAMX test followed NASA wind tunnel model test criteria for the design and checkout of the test stand and blades. However, the experimental blades can only be spun at reduced pressure, and thus must only be spun in the PAL facility. The static blade pull test demonstrated that the blades could handle the centrifugal loading of 110% RPM. In addition to the static testing, the first time the experimental blades were spun in the PAL, ballistic shields were installed around the test stand and the blades were spun to 110% of the desired test RPM to validate their structural integrity. Once the blades were rated to 110% of maximum testing RPM, the shields were

**Fig. 22 Ground vibration test for ROAMX test stand in PAL.**

removed so the aerodynamics were not impacted.

Prior to testing with blades, aerodynamic tares were collected at the testing RPMs. This was done to characterize the torque load required to spin all of the hardware except for the blades, so that the tare could be subtracted from the measured torque with blades installed. As expected, thrust load cells do not see loading at any RPM without blades, so only a torque tare is applied.

Discrete collective angles were tested for each run. Data was acquired at each discrete collective angle at $M_{tip} = 0.74$ for Ingenuity and $M_{tip} = 0.74$ and $M_{tip} = 0.8$ for ROAMX.

Data was acquired continuously throughout each run, which consisted of an RPM sweep at a set collective angle. Zero points were taken at the beginning and end of each run to account for temperature drift throughout the run. Data was collected for a minimum of 5 seconds at each dwell RPM (which represents between 275-300 revolutions collected) and RPM data points were taken sweeping up and back down. Collectives ranging from 3.9-10 degrees for the ROAMX blades and 8.4-19.4 degrees for the Ingenuity blades were tested.

At the PAL, Mars-pressure testing windows are typically limited to 40–60 minutes per SVS operating day. The ability for the PAL to pump down with the SVS is dependent on the SVS schedule availability. Usually, one pump down to Mars pressures is possible per day, because of the time it takes to bring the 4,000 cubic meter facility to Mars densities, conduct the experiment, and bring the facility back to one atmosphere. Because of the limitation on PAL pump down availability, the number of collective angles that can be acquired is limited. Future testing will include remote collective control to allow the ability to change the collective while at Mars pressures. However, currently the stand collective is manually changed before each test and held at a single discrete collective for the duration of a test run. The conditions that were tested are summarized in Table 3.

**Table 3 Experimental Test Conditions.**

| Parameter | ROAMX | Ingenuity |
|---|---|---|
| Density [kg/m$^3$] | 0.009, 0.015, 0.023 | 0.009, 0.015, 0.023 |
| Collective [°] | 3.9, 6.4, 8.1, 10.0 | 8.4, 10.5, 13.0, 16.0, 19.4 |
| RPM | 3300, 3600 | 3300 |
| Tip Mach Number | 0.74, 0.80 | 0.74 |

As part of the pre-test and post-test checklist, the sensors used to measure performance were checked with calibrated check loads and RCALS before and after each day of testing (meaning at each collective value tested) to ensure accuracy. The check load procedure consists of placing a known weight on the system and ensuring the load cells accurately measure the weight. The RCAL consists of placing a known resistance across the sensor and measuring the output voltage. These checks ensured that nothing changed for the sensors before, during, or after a test.

## B. Data Post-Processing

The AstroNova TMX data acquisition system output files were converted to comma separated value (.csv) files and Python was used to post-process the data. The post-processing code automatically identifies continuous regions where the RPM is steady and takes averages of the performance data [28]. Within the windows of steady RPM, the regulation is better than 1%, as seen in Figure 23.

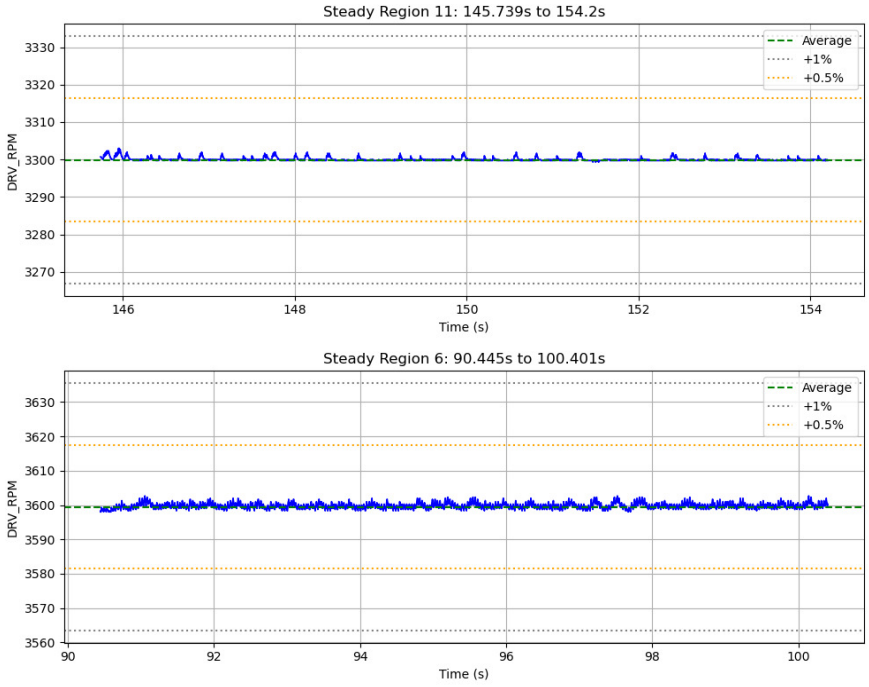


**Fig. 23 Example data collected at 3300 and 3600 RPM, demonstrating the steady RPM in those regions.**

As mentioned above, zero points were taken at the beginning and end of each run. Because of the water-cooled motor, the temperature of the sensors within each run remained mostly steady. However, a linear interpolation using time and beginning and end zero points was used to take into account any drift by the sensors used to measure performance during the run. The beginning and end zero linear interpolation was subtracted from each data point. The aerodynamic tares that were taken were found to have a linear fit as a function of RPM. Thus, in addition to the zero linear interpolation, the aerodynamic tares were subtracted as a function of RPM for each data point for the torque measurements. As stated above, there was no change in thrust found from the aerodynamic tare measurements; therefore, the beginning and end zero linear interpolation was applied for the thrust load cells, but no aerodynamic tares were applied. Once the zeroes and tares were subtracted from the data, the total thrust values ($T$) from the three separate thrust load cells were summed to determine the total thrust for each data point. This sum, along with the torque value ($Q$) for each data point, was used to calculate the rotor performance parameters, including coefficient of thrust ($C_T$), coefficient of power ($C_P$), power ($P$), blade loading ($\frac{C_T}{\sigma}$), and FM.

$$C_P = \frac{P}{\rho A (R\Omega)^3} \tag{1a}$$

$$C_T = \frac{T}{\rho A (R\Omega)^2} \tag{1b}$$

$$P = Q\Omega = C_P \, \rho A R^3 \Omega^3 \tag{1c}$$

$$FM = \frac{C_T^{3/2}}{\sqrt{2} C_P} \tag{1d}$$

where $\sigma$ is the solidity of the rotor, $\rho$ is the air density, $R$ is the rotor radius, $A$ is the rotor disk area, and $\Omega$ is the rotational velocity of the rotor in radians per second.

## V. Experimental Results and Discussion

Following the procedure described in Section IV, thrust and torque performance data was collected for the ROAMX and Ingenuity rotors. Note that the results here are for a four-bladed single rotor to allow for consistent comparison with the ROAMX blades and are not comparing to Ingenuity as flown on Mars or as tested at JPL. The design density for both rotors is $\rho = 0.015\ \frac{kg}{m^3}$.

Figure 24 shows hover performance results for the full-scale ROAMX rotor and full-scale Ingenuity rotor at their design density. Design tip speed for the ROAMX rotor is $M_{tip} = 0.8$ whereas Ingenuity's design tip speed is $M_{tip} = 0.7$. ROAMX results are shown at both $M_{tip} = 0.74$ and $M_{tip} = 0.8$ to compare directly to Ingenuity and show the performance without the benefit of higher tip speed. The ROAMX blades incorporate airfoils that were designed to mitigate compressibility effects seen at higher tip Mach numbers, and Figure 24 shows that there are no detrimental effects at higher tip speed for the ROAMX blades. Conversely, the ROAMX blades have improved performance at $M_{tip} = 0.8$ compared to $M_{tip} = 0.74$.

As discussed in Section II.D and II.F, several design elements can be improved to achieve superior blade performance for Mars, including utilizing airfoils that exhibit better performance, increasing the solidity of the rotor, and spinning the blades at higher tip speed. The plot of FM versus $\frac{C_T}{\sigma}$ in Figure 24c normalizes the blade performance with solidity to demonstrate the improvements in blade performance due to the increase in performance from improved airfoil technology. FM versus $C_T$ in Figure 24b, where the blades are not normalized by $\sigma$, shows the increase in blade performance from all aspects, highlighting the importance of the combination of factors in increasing blade performance. This also highlights the need for continued research into Mars helicopter rotors with higher solidities.

Figures 24b and 24c show that mean peak FM achieved for the ROAMX rotor at $M_{tip} = 0.74$ and $\rho = 0.015\ \frac{kg}{m^3}$ is 0.558, whereas mean peak FM for the Ingenuity rotor at the same $M_{tip}$ and $\rho$ is 0.445. This represents a 25% increase in FM. If the ROAMX rotor performance is taken at its design tip speed of $M_{tip} = 0.8$, the mean peak FM is 0.574, which represents a 29% increase over mean peak FM for the Ingenuity rotor.

Figures 24a, 24d, and 24e show that the ROAMX rotors requires less power and torque than the Ingenuity rotor to achieve the same thrust, for all data points and at all tip speeds. With increasing thrust, the Ingenuity rotor requires progressively more power for the same gain in thrust, compared to the ROAMX rotor. This echoes the results shown in [11], which shows that the roamx-0201 airfoils require less power than the Ingenuity clf5605 airfoils to generate the same amount of thrust.

Comparisons between the ROAMX and Ingenuity rotors are also shown for three separate atmospheric density conditions in Figure 25. Density of 0.015 kg/m$^3$ is the design density condition for the Ingenuity rotor and for the ROAMX rotor; densities of 0.009 kg/m$^3$ and 0.023 kg/m$^3$ represent the low and mid-high range of densities that a helicopter would fly at on Mars, to characterize blade performance at a range of Reynolds numbers.

More missions and capabilities for Mars helicopters are unlocked if the performance of the helicopter is not significantly impacted by different density/Reynolds number conditions. A change in density from 0.023 kg/m$^3$ to 0.009 kg/m$^3$ is a 61% reduction in density and thus Reynolds number. Table 4 shows the changes in mean peak FM with decreasing density (and thus Reynolds number), and shows that the ROAMX blade peak FM is less sensitive to decreasing Reynolds number. The mean peak FM of the ROAMX rotor at its design condition of $\rho = 0.015\ \frac{kg}{m^3}$ is 0.574; the mean peak FM of the ROAMX rotor at $\rho = 0.023\ \frac{kg}{m^3}$ is 0.608. For the Ingenuity rotor at $\rho = 0.015\ \frac{kg}{m^3}$ and $\rho = 0.023\ \frac{kg}{m^3}$, the mean peak FM are 0.445 and 0.510, respectively. The Ingenuity rotor decreases in FM by 0.065, whereas the ROAMX rotor decreases by half of that, indicating that the ROAMX rotor is less sensitive to changes in Reynolds number than the Ingenuity rotor.

**Table 4 Mean peak FM % Change with Decreasing Density at Design Speed (ROAMX $M_{\text{tip}} = 0.8$; Ingenuity $M_{\text{tip}} = 0.74$).**

| **Density (kg/m$^3$)** | **ROAMX** (%) | **Ingenuity** (%) |
|---|---|---|
| 0.009 | -11.2 | -18.5 |
| 0.015 | -5.6 | -12.8 |
| 0.023 | Baseline | Baseline |

As shown in Section II.E, results from wind tunnel testing, OVERFLOW, and PyFR DNS show that the roamx-0201 airfoil does indeed perform better than the Ingenuity clf5605 airfoil at all angles of attack, with up to 25% increase in lift possible [11]. Similarly for the experiment shown here, the ROAMX optimized blade using the roamx-0201 airfoil

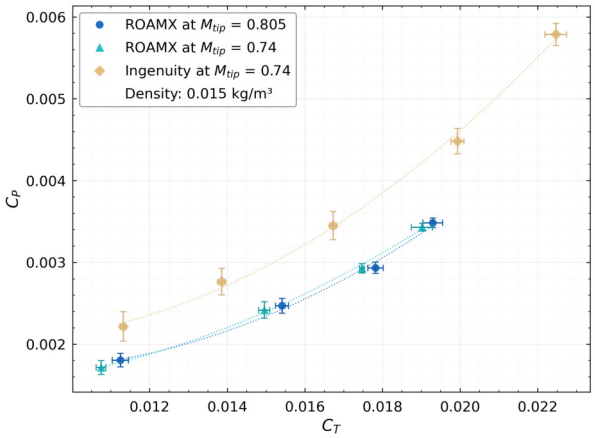


**(a) $C_P$ versus $C_T$.**

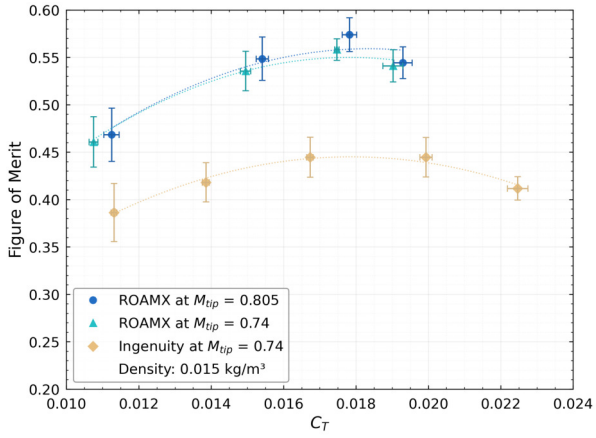


**(b) Figure of Merit versus $C_T$.**

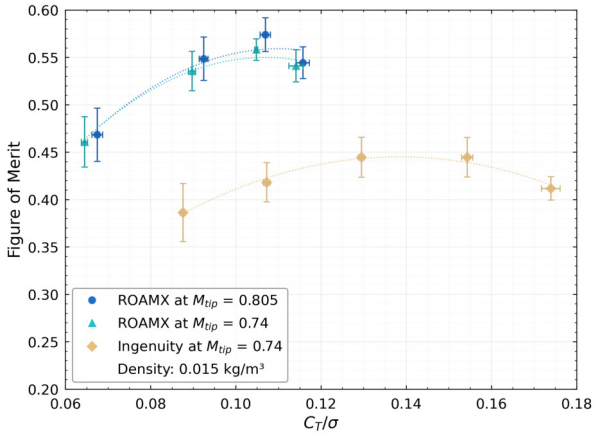


**(c) Figure of Merit versus $C_T/\sigma$.**

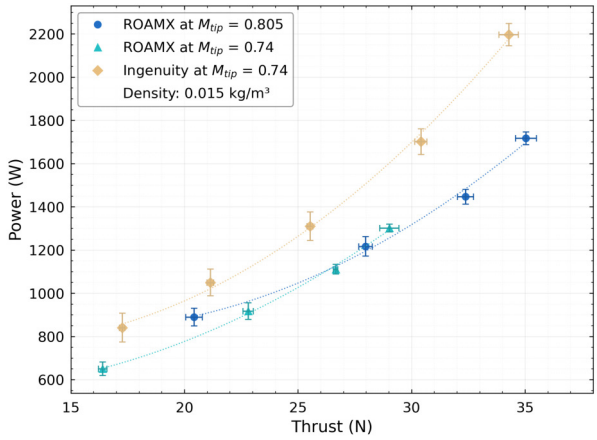


**(d) Power versus thrust.**

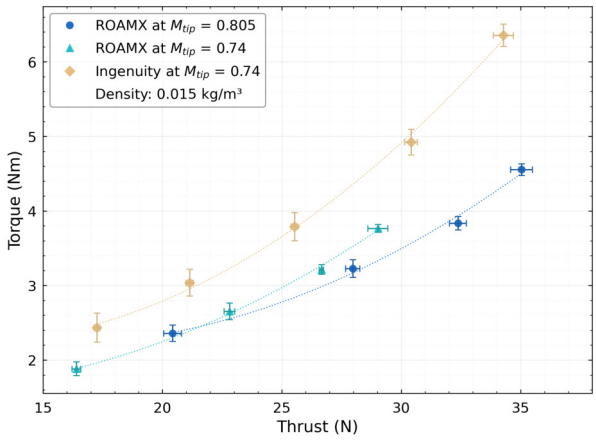


**(e) Torque versus thrust.**

**Fig. 24 Performance results at $\rho = 0.015\ \frac{kg}{m^3}$ for the Ingenuity blade at $M_{\text{tip}} = 0.74$ and for the ROAMX blade at $M_{\text{tip}} = 0.74$ and $M_{\text{tip}} = 0.8$).**

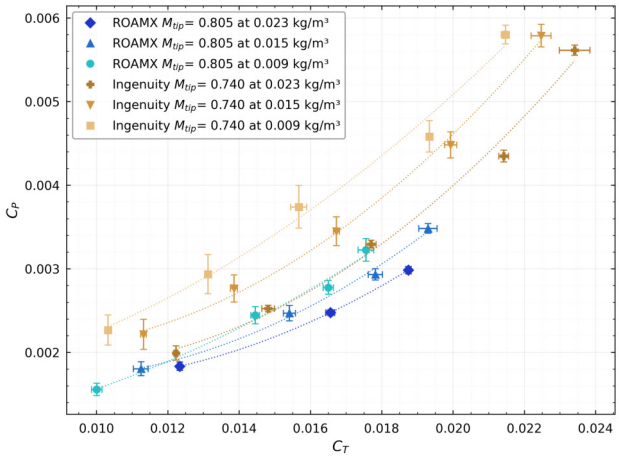


**(a) $C_P$ versus $C_T$ for ROAMX and Ingenuity blades.**

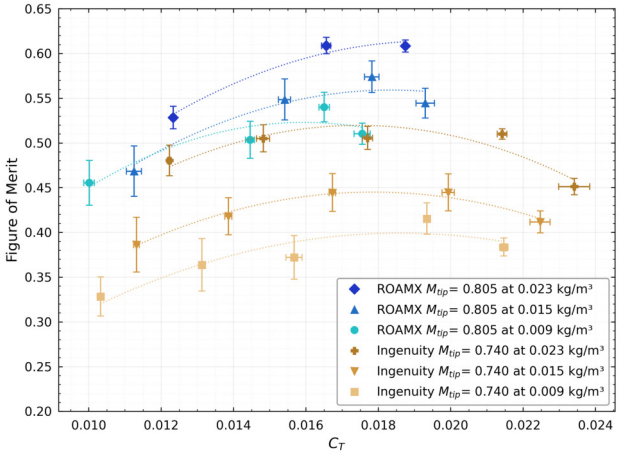


**(b) Figure of Merit versus $C_T$ for ROAMX and Ingenuity blades.**

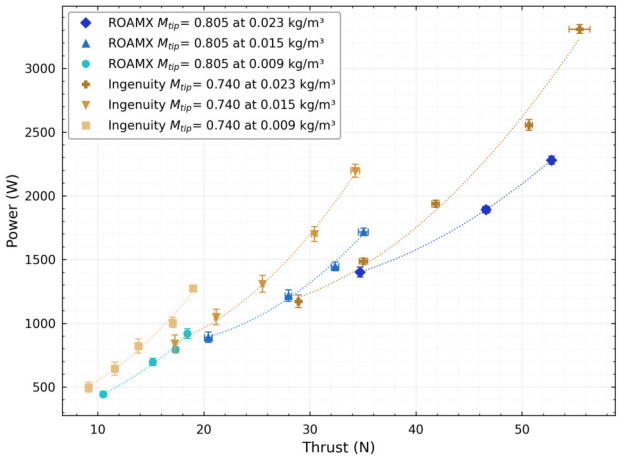


**(c) Power versus thrust for ROAMX and Ingenuity blades.**

**Fig. 25 Performance plots for ROAMX and Ingenuity blades at three discrete densities at their respective design tip speeds.**

demonstrates superior performance compared to the Ingenuity blade using the clf5605 airfoil, with 29% increase in peak FM possible at the design density and lower observed impact on performance with decreasing Reynolds number.

As implied from UMD studies, the authors believe that the blade experiences elastic deflection during experimental testing; studies by UMD concluded that extremely thin blades would experience the trapeze effect, which will try to untwist the blade, as well as propeller moment, which will try to flatten the blade [16]. The study in [16] found that the trapeze effect and propeller moment would roughly cancel each other out for the ROAMX blades, but only at certain collectives. An indication that there may be additional elastic twisting beyond what was predicted is that in the experiment, the ROAMX blades demonstrated higher performance than expected at low collectives and reached peak FM at a lower $\frac{C_T}{\sigma}$ than expected. This difference in performance could also be attributed to vibrations that occur in full-scale testing that could be different than the steady aerodynamics that are used to predict the performance. Because of the OVERFLOW (approaching ILES), PyFR DNS, and experimental wind tunnel results from the Tohoku airfoil study [11], there is high confidence that the airfoil is performing as expected, and thus this effect is thought to be linked to the flexible deformations of the blade.

More research is needed to understand if and how the blade is deforming, including the impact of vibrations, and what could potentially be causing discrepancies between predicted and experienced angle of attack distributions along the blade. This could be achieved by including a high speed video camera recording of the blade during testing.

If the magnitude of the flexible deformation is understood and constant, pre-twist can be added to the blade design to ensure that the expected angle of attack is obtained during operation. The ROAMX airfoil technology benefits are also present with thicker airfoils, for which deformation is minimized, as seen in [9], and these thicker airfoils can be a choice for designers. A thicker airfoil was intentionally not selected for this first round of experimental testing, as this study is intended to test and develop a novel airfoil shape at the limits imposed by manufacturing (thickness of 1% of chord) to provide information and guidelines for future designers. Therefore, in the future, an integrated aeroelastic approach to design is crucial, the key elements of which were established by this project.

The results presented here would greatly benefit from follow-on fundamental aerodynamic computational and experimental research, including:

- Experimental testing of expanded test matrix including:
  - Additional collective angles;
  - Higher tip speeds;
  - Characterization of stall;
  - High speed video capabilities to observe potential deformation of the blades;
  - Additional flow visualization techniques.
- Investigation into further increases in airfoil and blade performance by:
  - Further research into novel airfoil shapes such as roamx-1301, which showed higher performance than the roamx-0201 airfoil which was chosen to demonstrate performance in the ROAMX project;

## VI. Summary

The ROAMX project sought to establish fundamental physics, numerical tools, key elements of design, and acquire benchmark data to support the development of larger, more capable helicopters for Mars. This was achieved through the following accomplishments:

- A novel lift generation technique was discovered and validated [7];
- An airfoil modeling and optimization approach tailored to Mars helicopter flight regimes was developed and demonstrated [4, 6];
- An optimal airfoil portfolio was designed for Mars flight [9];
- Airfoil performance predictions at Mars flight conditions were validated via wind tunnel testing and high-fidelity CFD [11, 29].
- A computational framework for airfoil and blade coupled optimization was developed and validated [4, 6];
- A structural design framework was established and validated for Mars flight applications, for which blade strength was validated by static pull test and spinning of the blades at 110% of the test RPM [15, 16, 22];
- NASA Ames facility enhancements were implemented to expand the experimental capabilities for Mars helicopters.
- A state-of-the-art high accuracy hover rotor test stand was developed and tested, and can be used for rapid testing of blade performance for future research or missions to Mars;
- Optimized blade performance at Mars flight conditions was demonstrated to achieve 29% higher peak FM than the baseline Ingenuity blades.

ROAMX blades were shown to perform better than the baseline Ingenuity blades (which use conventional airfoil shapes), requiring less power to achieve equivalent thrust. Sensitivities to changes in density and Reynolds number are shown to be lesser for the ROAMX blades than for the Ingenuity blades.

ROAMX airfoil technology is already being used for future generation Mars Helicopter mission concepts, such as Chopper, which is being developed at JPL and the Long-Range Mars Rotorcraft concept [12, 14].

Future work to continue to enable successful Mars helicopters includes:

- Forward flight and unsteady testing of Mars-optimized rotors at Mars aerodynamic conditions;
- Coupled aerodynamic and structural analysis in 3-dimensions for Mars rotor blades;
- Research and development of higher solidity rotors for Mars heavy lift vehicle applications.

Because of the ROAMX project, NASA now possesses validated aerodynamic, structural, and facility capabilities that are bringing to reality Mars rotorcraft that can fly farther, carry payloads, and substantially expand science and exploration on the Red Planet.

**Fig. 26 ROAMX test stand and team inside the PAL.**



## Acknowledgments

The ROAMX project is funded through the Early Career Initiative program within the Science Technology Mission Directorate at NASA.

The authors would like to thank Dr. William Warmbrodt, Dr. Michael LaPointe, and Carl Russell for their excellent leadership and support throughout the project. The NASA Ames Machine Shop, especially Vince Derilo, Joel Hernandez, Jon Sasaki, Rob Kornienko, Ron Hovland, and Marissa Melo are thanked. Niklas Beck, Michael Derderian, and Benjamin Franklin are thanked for their outstanding support. Jon-Pierre Wiens is thanked for the exceptional ROAMX team pictures. Larry Young is thanked for his continuous support. Tom Norman is thanked for sharing his 40+ years of experimental expertise. Tove Ågren and Patricia Ventura Diaz are thanked for their in-depth review of this paper.

**Fig. 27 ROAMX test stand and expanded team inside the Planetary Aeolian Laboratory.**

## References


[1] Koning, W. J. F., Johnson, W. R., and Grip, H. F., "Improved Mars Helicopter Aerodynamic Rotor Model for Comprehensive Analyses," *44th European Rotorcraft Forum*, Delft, The Netherlands, 2018. URL `https://rotorcraft.arc.nasa.gov/Publications/files/Koning_2018_TechMx.pdf`.

[2] Cummings, H. V., Perez Perez, B. N., Koning, W. J. F., Johnson, W. R., Young, L. A., Haddad, F. B., Romander, E. A., Balaram, J. B., Tzanetos, T., Bowman, J., Wagner, L. N., Withrow-Maser, S. N., Isaacs, E., Toney, S., Shirazi, D., Conley, S. A., Pipenberg, B. T., Datta, A., Lumba, R. T., Chi, C., Smith, J. K., Cornelison, C. J., Perez, A., Nonomura, T., and Asai, K., "Overview and Introduction of the Rotor Optimization for the Advancement of Mars eXploration (ROAMX) Project," *VFS Aeromechanics for Advanced Vertical Flight Technical Meeting*, Vertical Flight Society, San Jose, CA, 2022.

[3] NASA, "ROAMX Testing in the Planetary Aeolian Laboratory (PAL) at NASA Ames Research Center," `https://www.nasa.gov/general/roamx-testing-in-the-planetary-aeolian-laboratory-pal-at-nasa-ames-research-center/`, Mar. 2025. Accessed: 2025-08-09.

[4] Koning, W. J. F., Perez Perez, B. N., Cummings, H. V., Romander, E. A., and Johnson, W. R., "ELISA: A Tool for Optimization of Rotor Hover Performance at Low Reynolds Number in the Mars Atmosphere," *Vertical Flight Society Sixth Decennial Aeromechanics Specialists' Conference*, Vertical Flight Society, Santa Clara, CA, 2024.

[5] Johnson, W., Withrow-Maser, S., Young, L. A., Malpica, C., Koning, W. J. F., Kuang, W., Fehler, M., Tuano, A., Chan, A., Datta, A., Chi, C., Lumba, R., Escobar, D., Balaram, J., Tzanetos, T., and Grip, H. F., "Mars Science Helicopter Conceptual Design," NASA Technical Memorandum NASA/TM–2020–220485, National Aeronautics and Space Administration, Moffett Field, CA, 2020. URL `https://rotorcraft.arc.nasa.gov/Publications/files/MSH_WJohnson_TM2020rev.pdf`.

[6] Koning, W. J. F., Perez Perez, B. N., Cummings, H. V., Romander, E. A., and Johnson, W. R., "ELISA: A Tool for Optimization of Rotor Hover Performance at Low Reynolds Number in the Mars Atmosphere," *Journal of the American Helicopter Society*, Vol. 69, No. 4, 2024. https://doi.org/10.4050/JAHS.69.042005.

[7] Koning, W. J. F., Romander, E. A., Perez Perez, B. N., Cummings, H. V., and Buning, P., "On Improved Understanding of Airfoil Performance Evaluation Methods at Low Reynolds Number," *AIAA Journal*, 2023. https://doi.org/10.2514/1.C037023, URL https://rotorcraft.arc.nasa.gov/Publications/files/1.c037023.pdf.

[8] McGhee, R. J., Walker, B. S., and Millard, B. F., "Experimental Results for the Eppler 387 Airfoil at Low Reynolds Numbers in the Langley Low-Turbulence Pressure Tunnel," NASA Technical Memorandum 4062, National Aeronautics and Space Administration, 1988. URL https://ntrs.nasa.gov/api/citations/19890001471/downloads/19890001471.pdf.

[9] Koning, W. J. F., Perez Perez, B. N., Cummings, H. V., Romander, E. A., and Johnson, W. R., "Overview of Rotor Hover Performance Capabilities at Low Reynolds Number for Mars Exploration," *50th European Rotorcraft Forum*, Marseille, France, 2024.

[10] Witherden, F. D., Vincent, P. E., Trojak, W., Abe, Y., Akbarzadeh, A., Akkurt, S., Alhawwary, M., Caros, L., Dzanic, T., Giangaspero, G., Iyer, A. S., Jameson, A., Koch, M., Loppi, N., Mishra, S., Modi, R., Sáez-Mischlich, G., Park, J. S.,

Vermeire, B. C., and Wang, L., "PyFR v2.0.3: Towards industrial adoption of scale-resolving simulations," *Computer Physics Communications*, Vol. 311, 2025. https://doi.org/10.1016/j.cpc.2025.109567.

[11] Caros, L., Koning, W. J. F., Nagata, T., Asai, K., Buxton, O., Perez Perez, B. N., Romander, E. A., Nonomura, T., Cummings, H. V., and Vincent, P., "Computational and Experimental Comparison of CLF5605 and roamx-0201 Martian Helicopter Rotor Airfoils," , 2025. URL https://arxiv.org/abs/2511.14934.

[12] Withrow-Maser, S., Johnson, W. R., Koning, W. J., Ågren, T. S., Sahragard-Monfared, G., Bowman, J. S., Kaweesa, D. V., Ruan, A. W., Malpica, C. Z., Jones-Wilson, L. L., Izraelevitz, J., Delaune, J. H., Mier-Hicks, F., Ainza Sneeder, K. D., and Veismann, M., "Critical Aerodynamic and Performance Upgrades to Enable Larger Mars Rotorcraft Such as the Chopper Platform," *Proceedings of the Vertical Flight Society's 81st Annual Forum and Technology Display*, Virginia Beach, VA, USA, 2025. https://doi.org/10.4050/F-0081-2025-0388.

[13] Lee, P., Loya, D., Shubham, S., Colaprete, A., and Pacher, T., "Nighthawk: Rationale for a Mars Chopper Class Rotorcraft to Explore Noctis Labyrinthus," *56th Lunar and Planetary Science Conference (LPSC)*, The Woodlands, Texas, USA, 2025.

[14] Cornelius, J., Peters, N., Aires, J., Ågren, T., Lugo, D. N., Comer, A., and Miles, Z., "Long-Range Mars Rotorcraft Design Optimization using Machine Learning," *Proceedings of the Vertical Flight Society's 81st Annual Forum & Technology Display*, 2025. https://doi.org/10.4050/F-0081-2025-364, URL https://rotorcraft.arc.nasa.gov/Publications/files/Cornelius_LRMR_f81.pdf.

[15] Datta, A., "X3D — A 3-D Solid Finite Element Multibody Dynamic Analysis for Rotorcraft," *AHS Technical Meeting on Aeromechanics Design for Vertical Lift*, American Helicopter Society, San Francisco, CA, 2016.

[16] Lumba, R. T., Chi, C., Datta, A., Koning, W. J. F., Perez Perez, B. N., and Cummings, H. V., "Structural Design and Aeromechanical Analysis of Unconventional Blades for Future Mars Rotorcraft," *Journal of the American Helicopter Society*, Vol. 68, 2023. https://doi.org/10.4050/JAHS.68.042003.

[17] Datta, A., Patil, M., and Staruk, W., "Loads and Stresses on the Mars Helicopter Ingenuity Rotor," *Vertical Flight Society Sixth Decennial Aeromechanics Specialists' Conference*, Vertical Flight Society, Santa Clara, CA, 2024.

[18] Escobar, D., Chopra, I., and Datta, A., "High-Fidelity Aeromechanical Analysis of Coaxial Mars Helicopter," *Journal of Aircraft*, Vol. 58, No. 3, 2021, pp. 609–623. https://doi.org/10.2514/1.C035895.

[19] Sutherland, J., and Datta, A., "Fabrication, Testing, and 3D Comprehensive Analysis of Swept-Tip Tiltrotor Blades," *Journal of the American Helicopter Society*, Vol. 68, No. 1, 2023, pp. 1–17. https://doi.org/10.4050/JAHS.68.012002.

[20] Chi, C., Datta, A., Chopra, I., and Chen, R., "Three-Dimensional Strains on Twisted and Swept Composite Rotor Blades in Vacuum," *Journal of Aircraft*, Vol. 58, No. 1, 2021, pp. 1–16. https://doi.org/10.2514/1.C035746.

[21] Chi, C., Lumba, R., Su Jung, Y., and Datta, A., "Aeromechanical Analysis of a Next-Generation Mars Hexacopter Rotor," *Journal of Aircraft*, Vol. 59, No. 6, 2022, pp. 1463–1477. https://doi.org/10.2514/1.C036739.

[22] Wagner, L. N., Chan, A., Radotich, M. T., Perez Perez, B. N., Koning, W. J. F., and Cummings, H. V., "Blade Pull Test of the ROAMX Optimized Rotor Blade," NASA Technical Memorandum NASA–TM–20250008371, National Aeronautics and Space Administration, Ames Research Center, Moffett Field, CA, Aug. 2025.

[23] NASA Ames Research Center, Thermophysics Facilities Branch, "Planetary Aeolian Laboratory (PAL)," https://www.nasa.gov/thermophysics-facilities-branch-planetary-aeolian-laboratory/, 2023. Accessed: 2025-08-07.

[24] Perez Perez, B. N., "Forward Flight Rotor Performance at Martian Atmospheric Densities and Sensitivity to Low Reynolds Numbers," *Proceedings of the Aeromechanics for Advanced Vertical Flight Technical Meeting*, Vertical Flight Society, San Jose, CA, USA, 2020. URL https://rotorcraft.arc.nasa.gov/Publications/files/Brenda_Natalia_Perez_Perez_TVF_2020.pdf, presented January 21–23, 2020.

[25] Delaune, J., Izraelevitz, J., Young, L. A., Rapin, W., Sklyanskiy, E., Johnson, W., Schutte, A., Fraeman, A., Scott, V., Leake, C., Ballesteros, E., Withrow, S., Bhagwat, R., Cummings, H., Aaron, K., Veismann, M., Wei, S., Lee, R., Pabon Madrid, L., Gharib, M., and Burdick, J., "Motivations and Preliminary Design for Mid-Air Deployment of a Science Rotorcraft on Mars," *AIAA ASCEND 2020*, American Institute of Aeronautics and Astronautics, Virtual Event, 2020. https://doi.org/10.2514/6.2020-4030, URL https://arc.aiaa.org/doi/abs/10.2514/6.2020-4030.

[26] DUC Hélices, "Certificates and Approvals," https://www.duc-helices.com/en/our-certificates-and-approvals, 2025. Accessed Nov. 20, 2025.

[27] Anyoji, M., Numata, D., Nagai, H., and Asai, K., "Effects of Mach Number and Specific Heat Ratio on Low-Reynolds-Number Airfoil Flows," *AIAA Journal*, Vol. 53, No. 6, 2015, pp. 1640–1654. https://doi.org/10.2514/1.J053468.

[28] Perez Perez, B. N., Cummings, H. V., and Koning, W. J. F., "Data Report for the Rotor Optimization for the Advancement of Mars eXploration (ROAMX) Hover Test," NASA Technical Memorandum NASA–TM–20250010259, National Aeronautics and Space Administration, Ames Research Center, Moffett Field, CA, Nov. 2025.

[29] Koning, W. J. F., Perez Perez, B. N., Cummings, H. V., Nagata, T., Kanzaki, Y., Kasai, M., Miyagi, M., Nonomura, T., Asai, K., Caros Roca, L., Buxton, O., and Vincent, P., "Experimental Results for Mars Rotorcraft Airfoils (roamx-0201 and clf5605) at Low Reynolds Number and Compressible Flow in a Mars Wind Tunnel," NASA Technical Memorandum NASA–TM–20240004230, National Aeronautics and Space Administration, Ames Research Center, Moffett Field, CA, Apr. 2024. URL https://rotorcraft.arc.nasa.gov/Publications/files/NASA-TM-20240004230.pdf.